polymorphisms of genes. Quite a few numbers of association studies have been done with so-called candidate gene approaches [4] and genome-wide approaches [5]. Polymorphisms of many genes were shown to have significant association with BMD. However, the contribution of each gene in determining BMD is small and the result is not always reproducible [6,7]. One of the ways to circumvent the problems and to make outcome biologically and clinically relevant would be to use polymorphisms whose functional variations can be studied.

The vitamin-K-dependent gamma-glutamyl carboxylase (GGCX or VKGC; EC 6.4.-.-) is a microsomal enzyme and is necessary for post-translational modification of vitamin-K-dependent proteins to exert their functions. The genomic structure of GGCX was elucidated in 1997 [8]. Concurrent with conversion of glutamate residue (Glu) to gamma-carboxyl glutamate residue (Gla), vitamin K hydroquinone is oxidized to vitamin K 2,3-epoxide by GGCX, then vitamin K 2,3-epoxide is reduced to vitamin K hydroquinone by vitamin K2,3-epoxide reductase (VKOR) [9]. In addition to vitamin-K-dependent coagulation factors, growth arrest-specific protein (gas6), proline-rich Gla protein-1 (PRGP-1), PRGP-2, bone Gla protein (BGP=osteocalcin) and matrix Gla protein (MGP) are also vitamin-K-dependent proteins [10]. BGP and MGP are abundant in bones [11] and assumed to play important roles in bone metabolism. Therefore, variation in the quality, i.e., carboxylation status, as well as the quantity of these proteins may contribute to variations in the susceptibility of individuals to osteoporosis and other skeletal disorder.

It is reported that the rare mutations of GGCX gene with amino acid substitution (Leu395Arg, Trp501Ser) cause consequential abnormal enzymatic activity, and these lead to vitamin-K-dependent protein defects and severe bleeding disorders [12,13]. However, any association between common variants of the GGCX gene with diseases has not been investigated. In addition, there have been no report comparing the function of products from the polymorphic genes. In this study, we compared the carboxylase activity of the products of the GGCX gene with each non-synonymous SNP and conducted association studies with forearm BMD according to the "common disease, common variant hypothesis" [14].

Materials and methods

Subjects

DNA samples were obtained from peripheral blood of 500 postmenopausal Japanese women living in an area of Japan. Mean ages with SD were 73.6± 5.7 years (range 65–90 years). None of the subjects were under the treatment with Warfarin.

All subjects were non-related volunteers and provided informed consent before the study. No participant had medical complications or was undergoing treatment for conditions known to affect bone metabolism, such as pituitary diseases, hyperthyroidism, primary hyperparathyroidism, renal failure, adrenal diseases, or rheumatic diseases, and none were receiving estrogen replacement therapy. The BMD of the radial bone (expressed in g/cm^2) of each participant was measured by dual energy X-ray absorptiometry (DXA) using DTX-200 (Osteometer Meditech Inc., Hawthorne CA, USA). *Z* scores were calculated using installed software (DTX-200) on the basis of Japanese women and adjusted for body mass index (BMI) utilizing regression analysis.

The ethics committee of the Tokyo Metropolitan Geriatric Hospital approved this study according to the Declaration of Helsinki.

SNPs screening and genotyping

DNA samples were extracted from leukocytes in peripheral blood. SNP screening in the exons of the GGCX gene was conducted with DNA samples of randomly chosen 20 subjects. All of the exons of the GGCX gene were amplified by polymerase chain reaction (PCR) with primers designed as reported previously [15]. Then, denaturing high performance liquid chromatography (DHPLC) with WAVE (Transgenomic Japan, Tokyo, Japan) was used to detect SNPs [16]. The detected variations in the PCR products were validated by direct sequencing utilizing Gene Rapid (Amersham Biosciences Corp, Piscataway, NJ). Then, the genotyping was performed by WAVE.

Construction of human GGCX cDNA (c.8762=A and c.8762=G) expression plasmid

Human GGCX cDNA (c.8762=A) in p*CMV*5 was obtained from American Type Culture Collection (ATCC Number 68666, GenBank M81592) (Manassas, VA). Site-directed mutagenesis was performed with a QuickChange XL Site-Directed Mutagenesis Kit (Stratagene, LA Jolla, CA) to prepare GGCX cDNA (c.8762=G) in p*CMV*5. A pair of mutagenesis primers, 5′-TCCTACTGCCCCC-GAAGGTTGCAACAA-3′ and 5′-TTGTTGCAACCTTCGGGGGCAG-TAGGA-3′ (underlined nucleotides are the mutagenesis target) was used for this process. Direct sequencing of the full length of each c.8762=G and c.8762=A was performed utilizing Gene Rapid (Amersham Biosciences Corp, Piscataway, NJ) to ascertain the sequence. Then, the ligation to pcDNA3.1/V5-His/lacZ was performed.

Preparation of microsome fraction from COS-7 cells

Microsomal fraction was prepared from the transfected COS-7 cells as reported previously [17]. COS-7 cells cultured for 24 h were transfected with pcDNA3.1/V5-His/lacZ-GGCX (c.8762=A; 325Gln) or pcDNA3.1/V5-His/lacZ-GGCX (c.8762=G; 325Arg) using the LipofectAMINE (Invitrogen Corp., Carlsbad, CA). The transfected cells were cultured for 5 days in 10% FBS D-MEM medium containing G418 300 μg/ml. The cells (5×10^7 cells) were washed with PBS (−) (calcium and magnesium free PBS), scraped and collected in PBS (−) containing 20% glycerol and 1× PIC (protease inhibitor cocktail: 2 mM dithiothreitol, 2 mM EDTA, 0.5 μg/ml leupeptin, 1 μg/ml pepstatin A, 2 μg/ml caprotinin). Cells were homogenized in a glass homogenizer (3×10 strokes) and centrifuged at 500×*g* for 7 min. The pellet was re-homogenized and washed 3 times with the same buffer. Pooled supernatants were centrifuged at 105,000×*g* for 1 h at 4°C to separate the microsomal fraction. The pellet was resuspended in PBS (−) containing 0.5% (w/v) CHAPS, 0.2% (w/v) phosphatidylcholine, 1× PIC and 20% (v/v) glycerol by sonication.

Carboxylase activity assays

Carboxylase activity was assayed by previously described methods [18–20]. FLEEL was purchased from Bachem (Philadelphia, PA). L-a-Phosphatidylcholine (type V-E) and CHAPS were from Sigma Aldrich Japan (Tokyo, Japan). Vitamin K_2 (menaquinone-4) was from Eisai Co., Ltd. (Tokyo, Japan). The peptide ProFIX19 which contains the sequence AVFLDHENANKILNRPKRY was synthesized by Genenet Co., Ltd. (Fukuoka, Japan). $NaH^{14}CO_3$ (specific activity, 58 mCi/mmol) was from Amarsham Biosciences Corp. (NJ).

The amount of $^{14}CO_2$ incorporated into exogenous substrates was measured in reaction mixtures at 125 μl containing substrate at the indicated concentration, 222 μM reduced vitamin K2 (vitamin KH_2), 16 μM propeptide ProFIX19, 1.4 mM $NaH^{14}CO_3$ (5 μCi), 25 mM MOPS (pH 7.0), 500 mM NaCl, 0.16% (w/v) phosphatidylcholine, 0.16% (w/v) CHAPS, 8 mM DTT and 0.8 M ammonium sulfate, unless stated otherwise. All of the assay components except for the microsomal fraction were prepared as a master mixture. $^{14}CO_2$ incorporation into peptide substrates for over 30 min was assayed in a scintillation counter. Stimulation experiments with vitamin KH_2 were performed at a constant concentration of the enzyme sample and substrate (3.6 mM FLEEL)

with increasing concentrations vitamin KH_2, as indicated. All assays were performed in quadruplicate.

Statistical analysis

The allele frequency, haplotype frequency and indices of linkage disequilibrium such as D, D' and r^2 were calculated by SNPAlyze ver3.2 Pro (DYNACOM, Tokyo, Japan). The Pearsons's goodness of fit test with one degree of freedom was used to examine Hardy–Weinberg equilibrium among GGCX genotypes.

The following analysis were performed by StatView 5.0 software (SAS Institute Inc., Cary, NC) and significance was defined as $p<0.05$. ANOVA was used to compare baseline characteristics (age, height, weight and BMI) among GGCX genotypes. The Mann–Whitney's U test was utilized to examine the effects of GGCX genotypes on BMI adjusted Z scores. The unpaired t-test was used to compare the carboxylase activity.

Results

SNP search and genotyping

Table 1 summarizes the SNPs detected in our SNP search. These were already registered in the dbSNP (http://www.ncbi.nlm.nih.gov/SNP/) (Table 1a) and each genotype showed Hardy–Weinberg equilibrium ($p>0.05$). The linkage disequilibrium coefficients, D' values, in c.8762 G>A, c.9167 C>T and c.9191 C>T were higher than 0.98, indicating that these three SNPs are in a strong linkage disequilibrium and constitute a haplotype block [21] (Table 1b). The genotype c.8762=AA perfectly corresponded to c.9167=TT, c.8762=AG to c.9167=CT and c.8762=GG to c.9167=CC, i.e., c.8762 G>A and c.9167 C>T were completely linked together. The SNP c.8762 G>A was a non-synonymous SNP, changing amino acid 325 Arg to Gln (Table 1a). Therefore, the genotypes were described as 325-Arg, 325-Arg/Gln, or 325-Gln afterward in this report. We focused on this non-synonymous polymorphism in further analyses. Genotype distribution in the subjects was as follows; 325-Arg=265, 325-Arg/Gln=203 and 325-Gln=32. The baseline characteristics (age, height, weight and BMI) were not significantly different among these genotypes (Table 2).

Table 1
Summary of GGCX SNPs

a. Detected SNPs

Name	Base position	Allele frequency	Amino acid change	dbSNP[a]
c.8762 G>A	8762 (exon8)	G:A=0.73:0.27	Arg325Gln	Rs699664
c.9167 C>T	9167 (exon9)	C:T=0.73:0.27	none (406Arg)	Rs2592551
c.9191 C>T	9191 (exon9)	C:T=0.93:0.07	none (414Thr)	Rs10179904

b. Tests for linkage disequilibrium between GGCX SNPs

SNP1	SNP2	SNP3	D	D'	r^2
c.8762 G>A	c.9167 C>T		0.195	1.000	1.000
c.8762 G>A		c.9191 C>T	−0.017	0.999	0.026
	c.9167 C>T	c.9191 C>T	−0.017	0.999	0.026

The D, D', and r^2 were calculated by SNPAlyze ver3.2 Pro.
The D' value was an absolute value ($0 \leqq D' \leqq 1$).
[a] Numbers are from dbSNP database of NCBI (http://www.ncbi.nlm.gov/SNP/).

Table 2
Baseline characteristics of subjects

Genotype	325-Gln	325-Arg/Gln	325-Arg	p value
Number	32	203	265	
Age	74.1±5.9	73.1±5.7	73.9±5.7	0.344
Height (cm)	144.4±5.0	144.8±5.9	145.3±5.7	0.534
Weight (kg)	48.7±5.6	50.4±8.7	51.1±8.2	0.265
BMI (kg/m^2)	23.3±2.4	24.0±3.5	24.2±3.4	0.409

Data were shown as mean±SD.
The p values were calculated by ANOVA.

Carboxylase activity

Efficient transfection into COS-7 cells was confirmed by measuring luciferase activity from co-transfected internal control vector (pRL-*CMV*) (data not shown). Moreover, production of GGCX by transfected COS-7 cells was visualized

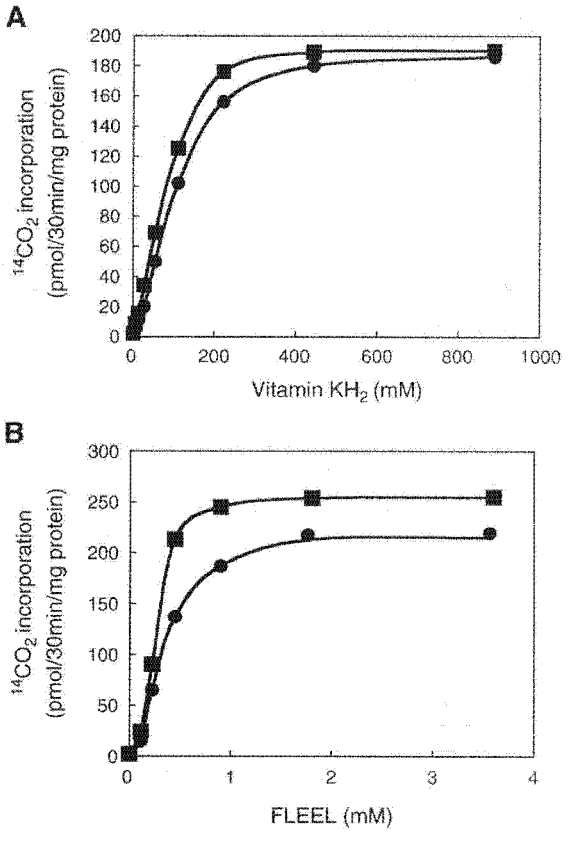

Fig. 1. Influence of vitamin KH_2 or FLEEL on the carboxylase activity of GGCX 325Gln or 325Arg. (A) Carboxylation of 3.6 mM FLEEL at vitamin KH_2 concentrations between 0 and 888 mM was measured by $^{14}CO_2$ incorporation for both 325Gln (filled squares) and 325Arg (filled circles). (B) Carboxylation in 222 mM vitamin KH_2 at FLEEL concentrations between 0 and 3.6 mM was measured by $^{14}CO_2$ incorporation for both 325Gln (filled squares) and 325Arg (filled circles).

as a 130 kDa band in Western blot analysis using antibodies to V5 and His (data not shown).

GGCX 325-Gln (c.8762=A) was determined to have a Km for vitamin KH_2 of 71.34±6.20 μM (mean±SD). The Km of GGCX 325-Arg (c.8762=G) for vitamin KH_2 was 90.31± 4.63 μM, about 1.3-fold higher than that of 325-Gln (p=0.029). The Vmax determined for 325-Arg (186±7.88 pmol/30 min/mg) was lower than that of 325Gln (191±9.45 pmol/30 min/mg) (p=0.033). The Vmax/Km for vitamin KH_2 with 325-Arg (2.06±0.12 pmol/30 min/mg/μM) was thus reduced by 24% compared with 325Gln (2.68±0.20 pmol/30 min/mg/μM) (p=0.032) (Fig. 1 and Table 3a).

Kinetic constants for FLEEL carboxylation were determined in the presence of saturating concentrations of ProFIX19. The Km of 325-Gln for FLEEL was 0.27±0.02 mM. The Km of 325-Arg for FLEEL was 0.32±0.03 mM, about 1.3-fold higher than that of 325-Gln (p=0.016). Comparison of Vmax for FLEEL carboxylation showed that the reaction rate of 325-Arg (215±5.28 pmol/30 min/mg) was about 1.2-fold slower than that of 325-Gln (255±6.33 pmol/30 min/mg) (p=0.011). The Vmax/Km for FLEEL with 325-Arg (671.9±10.79 pmol/30 min/mg/mM) was thus reduced about 30% compared with 325Gln (944.4±9.21 pmol/30 min/mg/mM) (p=0.018) (Fig. 1 and Table 3b). These results indicate that 325-Gln has higher carboxylase activity than 325-Arg.

Association study of BMD

The subjects with 325-Gln had the highest adjusted Z score but the difference was not statistically significant in all subjects; 0.297±0.866 (mean±SD), 0.030±0.959 and 0.057±0.882 for 325-Gln, 325-Arg/Gln, or 325-Arg, respectively. From this result, we assumed that the effect of GGCX polymorphism c.8762 G>A is allele G dominant, and compared 325-Gln vs. 325-Gln/Arg+325-Arg.

Table 3
Comparison of the kinetic parameters of GGCX 325-Gln and 325-Arg

a. Using vitamin KH_2 as a substrate

Substrate	Enzyme	Km (μM)	Vmax (pmol/30 min/mg)	Vmax/Km (pmol/30 min/mg/μM)
Vitamin KH_2 [a]	325Gln	71.34±6.20	191±9.45	2.68±0.20
	325Arg	90.31±4.63	186±7.88	2.06±0.12
p value		0.029	0.033	0.032

b. Using FLEEL as a substrate

Substrate	Enzyme	Km (μM)	Vmax (pmol/30 min/mg)	Vmax/Km (pmol/30 min/mg/mM)
FLEEL [b]	325Gln	0.27±0.02	255±6.33	944.4±9.21
	325Arg	0.32±0.03	215±5.28	671.9±10.79
p value		0.016	0.011	0.018

All assays were performed in quadruplicate.
Data were shown as mean±SD. The p values were calculated by the unpaired t-test.
[a] Determined at 3.6 mM FLEEL.
[b] Determined at 222 mM vitamin KH_2.

Table 4
Comparison of BMI-adjusted Z score of BMD among the genotypes of GGCX Arg325Gln

Genotype	325-Gln	325-Arg or 325-Arg/Gln	p value
All	0.297±0.866 (32)	0.045±0.915 (468)	0.132
<75	0.022±0.926 (18)	−0.017±0926 (275)	0.861
>75	0.650±0.883 (14)	0.133±0.650 (193)	0.038

The data are expressed as mean±SD.
The p values were calculated by the Mann–Whitney's U test.

The adjusted Z score seemed higher in the subjects with 325-Gln than those with other genotypes. However, the difference was not statistically significant (Table 4). Then we divided the subjects into two groups according to the age; above and below 75 years. As a result, the adjusted Z score in the subpopulation older than 75 years (n=207) was higher in those with 325-Gln (0.650±0.883, mean±SD) than those with 325-Gln/Arg or 325-Arg (0.133±0.064) (p=0.0383). On the other hand, this association was not found in the subpopulation younger than 75 years.

Discussion

This is the first report to demonstrate the different activities of GGCX between the common genotypes. Although the association study of these genotypes with BMD provided a statistically significant results, the limited size of the samples should make us cautious and modest and requires further studies. Because the site of the BMD measurement in this study was limited to the radius, the association of GGCX genotype with BMD of spine and proximal femur would be another important issue. In addition, low BMD does not explain all of the pathophysiology of bone fragility in osteoporotic patients. Our results would explain a part of BMD determinants not the osteoporosis of itself, and suggest that the GGCX gene polymorphism may be involved in the pathogenesis of osteoporosis.

The physiological roles of vitamin-K-dependent Gla proteins in bone metabolism have not been elucidated yet, but it was reported that under-carboxylated osteocalcin (ucOC) was negatively correlated with BMD [22] and that administration of vitamin K decreased ucOC and worked to increase BMD [23]. Another vitamin-K-dependent protein, MGP (matrix Gla protein) has been reported to be a regulator of calcification in several studies. For example, MGP-deficient mice exhibited inappropriate calcification of various cartilages including the growth plate, which eventually led to short stature [24]. In addition, it was suggested that under-carboxylated MGP was biologically inactive and may increase the risk for vascular calcification [25]. Therefore, properly carboxylated MGP is assumed to be necessary to protect vascular system from calcification and skeletal system from abnormal ossification [26]. People with 325-Gln might have a higher efficiency of carboxylation of these proteins with the given status of vitamin K, considering that carboxylase activity of 325-Gln was higher than that of 325-Arg *in vitro*. Because this variation of carboxylase activity between the genotypes was examined

using only a standard substrate, FLEEL, in this study, functional significance of the polymorphisms in physiological target molecules and tissues should be investigated further. For example, *in vitro* studies using other substrates as well as measurements of the serum levels and carboxylation status of vitamin-K-dependent proteins would be informative.

In order to be carboxylated, vitamin-K-dependent proteins are assumed to be bound specifically to 343–355 residues of GGCX with high affinity. Among these residues, 343 (Cys) and 345 (Tyr) were suggested to be located near the catalytic center [27]. Moreover, it was also reported that chemical modification of 323-Cys and 343-Cys decreased its carboxylase activity [28]. Considering a study of human GGCX membrane topology, human GGCX probably may span the endoplasmic reticulum membrane 5 times and the interval of fourth and fifth transmembrane region may be composed of amino acids 313–361 [29]. Since amino acids 323-Cys, 325-Arg/Gln, 343-Cys, 345-Tyr and 343–355 are involved in the interval of fourth and fifth transmembrane regions (313–361), the amino acid substitution of 325 residue (Arg/Gln) may affect enzymatic activity directly or indirectly through influencing the function of these residues.

The higher Km value of GGCX 325-Arg would mean that higher intake of vitamin K may cancel the effects of this genotype. Therefore, the influence of GGCX polymorphisms should be studied further from the viewpoints of gene–environment interactions as well as ethnic/race differences. When the association study with the GGCX gene polymorphism is designed among different ethnicities, the intake of vitamin Ks should be handled carefully, because there are large ethnic differences in vitamin K status as we reported previously [30]. On the other hand, the difference in Vmax between the 325-Gln and 325-Arg suggests that the GGCX polymorphism might affect the carboxylase activity at the pharmacological level of vitamin K and might contribute to the difference of individual sensitivity to vitamin K treatment for osteoporosis.

The reason for age-dependent effect of GGCX polymorphism is not obvious, but we reported the similar age-dependent effects of functional SNP in tissue non-specific alkaline phosphatase gene [31]. It is reported that dietary vitamin K intake decreases with age, and elevated levels of ucOC may result from subclinical vitamin K deficiency and are frequently observed in the elderly [32]. The administration of vitamin K increased osteocalcin's hydroxyapatite binding capacity, decreased urinary calcium and hydroxyproline excretion in postmenopausal women but no effect was observed in premenopausal women [33]. These evidences may explain partly that the effects of different carboxylase activity between 325-Gln and 325-Arg might become obvious in advancing aging.

In conclusion, we reported here for the first time the different activities of GGCX between the common genotypes which were associated with BMD in elderly Japanese women. There are two major limitations in this study as discussed above; the limited sample size and the lack of extensive functional studies. Further studies are absolutely necessary to delineate any conclusion regarding the GGCX polymorphism and osteoporosis.

Acknowledgments

This work was supported in part by the grants from the Japanese Ministry of Health, Labor and Welfare. We thank Ms. M. Kumasaka for her expert technical assistance.

References

[1] NIH. Consensus development panel on osteoporosis prevention, diagnosis, and therapy osteoporosis prevention, diagnosis, and therapy. JAMA 2001;285:785–95.
[2] Kanis JA. Diagnosis of osteoporosis and assessment of fracture risk. Lancet 2002;359:1929–36.
[3] Pocock NA, Eisman JA, Hopper JL, Yeates MG, Sambrook PN, Eberl S. Genetic determinants of bone mass in adults. A twin study. J Clin Invest 1987;80:706–10.
[4] Andrew T, Macgregor AJ. Genes and osteoporosis. Curr Osteoporos Rep 2004;2:79–89.
[5] Long JR, Xiong DH, Recker RR, Deng HW. The genetics of osteoporosis. Drugs Today (Barc) 2005;41:205–18.
[6] Pols HA, Uitterlinden AG. Genetic polymorphisms and clinical practice: the example of osteoporosis. Acta Clin Belg 2002;57:266–70.
[7] Shen H, Liu Y, Liu P, Recker RR, Deng HW, Nonreplication in genetic studies of complex diseases—Lessons learned from studies of osteoporosis and tentative remedies. J Bone Miner Res 2005;20:365–76.
[8] Wu SM, Stafford DW, Frazier LD, Fu YY, High KA, Chu K, et al. Genomic sequence and transcription start site for the human gamma-glutamyl carboxylase. Blood 1997;89:4058–62.
[9] Wu SM, Stanley TB, Mutucumarana VP, Stafford DW. Characterization of the gamma-glutamyl carboxylase. Thromb Haemost 1997;78: 599–604.
[10] Berkner KL. The vitamin K-dependent carboxylase. J Nutr 2000;130: 1877–80.
[11] Price PA. Gla-containing proteins of bone. Connect Tissue Res 1989;21: 51–7.
[12] Brenner B, Sanchez-Vega B, Wu S-M, Lanir N, Stafford DW, Solera J. A missense mutation in a gamma-glutamyl carboxylase gene causes combined deficiency of all vitamin K-dependent blood coagulation factors. Blood 1998;92:4554–9.
[13] Spronk HMH, Farah RA, Buchanan GR, Vermeer C, Soute BAM. Novel mutation in the gamma-glutamyl carboxylase gene resulting in congenital combined deficiency of all vitamin K-dependent blood coagulation factors. Blood 2000;96:3650–2.
[14] Doris PA. Hypertension genetics, single nucleotide polymorphisms, and the common disease: common variant hypothesis. Hypertension 2002;39: 323–31.
[15] Oldenburg J, von Brederlow B, Fregin A, Rost S, Wolz W, Eberl W, et al. Congenital deficiency of vitamin K dependent coagulation factors in two families presents as a genetic defect of the vitamin K-epoxide-reductase-complex. Thromb Haemost 2000;84:937–41.
[16] Hayward-Lester A, Oefner PJ, Sabatini S, Doris PA. Accurate and absolute quantitative measurement of gene expression by single-tube RT-PCR and HPLC. Genome Res 1995;5:494–9.
[17] Czerwiec E, Begley GS, Bronstein M, Stenflo J, Taylor K, Furie BC, et al. Expression and characterization of recombinant vitamin K-dependent gamma-glutamyl carboxylase from an invertebrate, Conus textile. Eur J Biochem 2002;269:6162–72.
[18] Ulrich MMW, Furie B, Jacobs M, Vermeer C, Furie BC. Vitamin K-dependent carboxylation. A synthetic peptide based upon the gamma-carboxylation recognition site sequence of the prothrombin propeptide is an active substrate for the carboxylation in vitro. J Biol Chem 1988;263:9697–702.
[19] Morris DP, Soute BAM, Vermeer C, Stafford DW. Characterization of the purified vitamin K-dependent gamma-glutamyl carboxylase. J Biol Chem 1993;268:8735–42.
[20] Mutucumarana VP, Stanfford DW, Stanley TB, Jin D, Solera J, Brenner B, et al. Expression and characterization of the naturally occurring

mutation L394R in human gamma-glutamyl carboxylase. J Biol Chem 2000;275:32572–7.
[21] Gabriel SB, Schaffner SF, Nguyen H, Moore JM, Roy J, Blumenstiel B, et al. The structure of haplotype blocks in the human genome. Science 2002;296:2225–9.
[22] Szulc P, Arlot M, Chapuy MC, Duboeuf F, Meunier PJ, Delmas PD. Serum undercarboxylated osteocalcin correlates with hip bone mineral density in elderly women. J Bone Miner Res 1994;9:1591–5.
[23] Shiraki M, Shiraki Y, Aoki C, Miura M. Vitamin K2 (menatetrenone) effectively prevents fractures and sustains lumbar bone mineral density in osteoporosis. J Bone Miner Res 2000;15:515–21.
[24] Luo G, Ducy P, McKee MD, Pinero GJ, Loyer E, Behringer RR, et al. Spontaneous calcification of arteries and cartilage in mice lacking matrix GLA protein. Nature 1997;386:78–81.
[25] Spronk HM, Soute BA, Schurgers LJ, Cleutjens JP, Thijssen HH, De Mey JG, et al. Matrix Gla protein accumulates at the border of regions of calcification and normal tissue in the media of the arterial vessel wall. Biochem Biophys Res Commun 2001;289:485–90.
[26] Shanahan CM, Proudfoot D, Farzaneh-Far A, Weissberg PL. The role of Gla proteins in vascular calcification. Crit Rev Eukaryot Gene Expr 1998;8:357–75.
[27] Pudota BN, Hommema EL, Hallgren KW, McNally BA, Lee S, Berkner KL. Identification of sequences within the gamma-carboxylase that represent a novel contact site with vitamin K-dependent proteins and that are required for activity. J Biol Chem 2001;276:46878–86.
[28] Tie JK, Jin DY, Loiselle DR, Pope RM, Straight DL, Stafford DW. Chemical modification of cysteine residues is a misleading indicator of their status as active site residues in the vitamin K-dependent gamma-glutamyl carboxylation reaction. J Biol Chem 2004;279:54079–87.
[29] Tie J, Wu SM, Jin D, Nicchitta CV, Stafford DW. A topological study of the human gamma-glutamyl carboxylase. Blood 2000;96:973–8.
[30] Kaneki M, Hodges S, Hosoi T, Fujiwara S, Lyons A, Cren ST, et al. Japanese fermented bean as the major determinant for the large geographical differences in circulating levels of vitamin K2 and its possible implication in hip fracture incidence. Nutrition 2001;17:315–21.
[31] Goseki-Sone M, Sogabe N, Fukushi-Irie M, Mizoi L, Orimo Hideo, Suzuki T, et al. Functional analysis of the single nucleotide polymorphisms 787T>C9 in the *Tissue-nonspecific alkaline phosphatase* gene associated with BMD. J Bone Miner Res 2005;20:773–82.
[32] Vermeer C, Jie KS, Knapen MH. Role of vitamin K in bone metabolism. Annu Rev Nutr 1995;15:1–22.
[33] Knapen MH, Hamulyak K, Vermeer C. The effect of vitamin K supplementation on circulating osteocalcin (bone Gla protein) and urinary calcium excretion. Ann Intern Med 1989;111:1001–5.

THE JOURNAL OF BIOLOGICAL CHEMISTRY VOL. 282, NO. 8, pp. 5736–5748, February 23, 2007

α-Synuclein Stimulates Differentiation of Osteosarcoma Cells

*RELEVANCE TO DOWN-REGULATION OF PROTEASOME ACTIVITY**

Received for publication, June 28, 2006, and in revised form, December 15, 2006 Published, JBC Papers in Press, December 22, 2006, DOI 10.1074/jbc.M606175200

Masayo Fujita[‡], Shuei Sugama[‡], Masaaki Nakai[‡], Takato Takenouchi[§], Jianshe Wei[‡], Tomohiko Urano[¶], Satoshi Inoue[¶], and Makoto Hashimoto[‡1]

From the [‡]Laboratory for Chemistry and Metabolism, Tokyo Metropolitan Institute for Neuroscience, Fuchu, Tokyo 183-8526, Japan, [§]Transgenic Animal Research Center, National Institute of Agrobiological Sciences, Tsukuba, Ibaraki 305-8634, Japan, and [¶]Department of Geriatrics and Gerontology, School of Medicine, University of Tokyo, Tokyo 113-8655, Japan

Because a limited study previously showed that α-synuclein (α-syn), the major pathogenic protein for Parkinson disease, was expressed in differentiating brain tumors as well as various peripheral cancers, the main objective of the present study was to determine whether α-syn might be involved in the regulation of tumor differentiation. For this purpose, α-syn and its non-amyloidogenic homologue β-syn were stably transfected to human osteosarcoma MG63 cell line. Compared with β-syn-overexpressing and vector-transfected cells, α-syn-overexpressing cells exhibited distinct features of differentiated osteoblastic phenotype, as shown by up-regulation of alkaline phosphatase and osteocalcin as well as inductive matrix mineralization. Further studies revealed that proteasome activity was significantly decreased in α-syn-overexpressing cells compared with other cell types, consistent with the fact that proteasome inhibitors stimulate differentiation of various osteoblastic cells. In α-syn-overexpressing cells, protein kinase C (PKC) activity was significantly decreased, and reactivation of PKC by phorbol ester significantly restored the proteasome activity and abrogated cellular differentiation. Moreover, activity of lysosome was up-regulated in α-syn-overexpressing cells, and treatment of these cells with autophagy-lysosomal inhibitors resulted in a decrease of proteasome activity associated with up-regulation of α-syn expression, leading to enhance cellular differentiation. Taken together, these results suggest that the stimulatory effect of α-syn on tumor differentiation may be attributed to down-regulation of proteasome, which is further modulated by alterations of various factors, such as protein kinase C signaling pathway and a autophagy-lysosomal degradation system. Thus, the mechanism of α-syn regulation of tumor differentiation and neuropathological effects of α-syn may considerably overlap with each other.

α-Synuclein (α-syn)[2] is a presynaptic protein that belongs to the syn family of peptides with two other members, β- and γ-syn (1, 2). These proteins are characterized by a native unfolded structure with a highly conserved N-terminal region and a divergent C-terminal acidic region (3). However, the most striking feature is that α-syn possesses a highly hydrophobic domain in the middle region that was previously purified from Alzheimer disease brain amyloid (4). Due to this hydrophobic domain, α-syn forms toxic protofibrils that might cause synaptic injury and dysfunction (5). The importance of α-syn in the pathogenesis of neurodegenerative disorders was further augmented by identification of missense mutations of α-syn in familial Parkinson disease (PD) (6–8). Subsequently, numerous histological studies have shown that α-syn is a major constituent in Lewy bodies and dystrophic neuritis in sporadic PD and diffuse Lewy body disease (2). Immunoreactivity of α-syn was also shown in glial cell inclusions in multiple system atrophy (2). By contrast, β-syn, which lacks the majority of the hydrophobic domain in the middle region, was protective against protofibrils of α-syn (9, 10). Thus, these results support the contention that α- and β-syn may play a central role in the pathogenesis of neurodegenerative diseases.

On the other hand, γ-syn, the less conserved third member of the syn family of peptides, was identified as a breast cancer-specific gene product (11) and has been extensively studied in a variety of cancers, such as breast cancer, ovarian cancer, liver cancer, pancreatic adenocarcinoma, and bladder cancer (11–15). Because expression levels of γ-syn were well correlated with the presence of metastatic lesions, it has been generally thought that γ-syn might regulate tumor invasiveness and metastasis (16, 17). Several studies indicated that γ-syn might be involved in the deregulation of cell cycle in cancer. For example, γ-syn interacted with a mitotic spindle checkpoint protein, BubR1, leading to decreased checkpoint function and tumor progression (18, 19). Moreover, γ-syn stimulated cell proliferation by augmenting estrogen receptor-mediated signaling in breast cancer cells (20). Thus, the role of γ-syn has been investigated mainly in the area of tumor biology.

* This work was supported in part by a grant-in-aid for Science Research from the Ministry of Education, Culture, Sports, Science, and Technology, Japan and a project grant from Tokyo Metropolitan Organization. The costs of publication of this article were defrayed in part by the payment of page charges. This article must therefore be hereby marked "*advertisement*" in accordance with 18 U.S.C. Section 1734 solely to indicate this fact.

[1] To whom correspondence should be addressed: Laboratory for Chemistry and Metabolism, Tokyo Metropolitan Institute for Neuroscience, 2–6 Musashidai, Fuchu, Tokyo 183-8526, Japan. Tel.: 81-42-325-3881; Fax: 81-42-321-8678; E-mail address: mhashimoto@tmin.ac.jp.

[2] The abbreviations used are: syn, synuclein; PD, Parkinson disease; UPS, ubiquitin-proteasome system; PKC, protein kinase C; PMA, 12-myristate 13-acetate; 4αPDD, 4α-phorbol 12,13-didecanoate; 3-MA, 3-methyladenine; Rb, retinoblastoma; RT, reverse transcriptase; CAPS, 3-(cyclohexylamino)-1-propanesulfonic acid; LSCM, laser-scanning confocal microscope; ALP, alkaline phosphatase; PBS, phosphate-buffered saline; LSCM, laser-scanning confocal microscope.

A recent study, however, suggests that molecular pathways shared by neurodegenerative disease and cancer may be considerably overlapped than thought before. Supporting this notion, it has been recently shown that several familial PD-causing factors are involved in the pathogenesis of cancer (21). First, overexpression of the PARK2 parkin, which functions as an E3 ligase in the ubiquitin-proteasome system (UPS), resulted in growth suppression in hepatocellular carcinoma cells (22). Furthermore, ectopic expression of parkin reportedly reduced *in vivo* tumorigenesis in nude mice (23). Second, the PARK5 ubiquitin C-terminal hydrolase light chain-1, which acts as a de-ubiquitinating enzyme in UPS, was shown to suppress proliferation of a lung cancer cells (24). Other evidence suggests that ubiquitin C-terminal hydrolase light chain-1 might be involved in the degradation of p27, a cyclin-dependent kinase inhibitor (25). Third, the PARK7 DJ-1 was first identified as an oncogene product that stimulated transformation of NIH3T3 cells in coordination with Ras (26). DJ-1 was recently shown to up-regulate the phosphatidylinositol 3-kinase pathway through inhibition of the tumor suppressor phosphatase PTEN, leading to enhance survival of cancer (27).

In the same context one may wonder if α- and β-syn, the central players in the pathogenesis of PD, might play some important roles for the regulation of cancer. Indeed, α-syn was widely expressed in a variety of brain tumors, such as medulloblastoma, neuroblastoma, pineoblastoma, and ganglioma (28, 29). Furthermore, both α- and β-syn were shown to be expressed in the peripheral cancers, including ovarian and breast cancers (30). Although the role of syn proteins in the pathogenesis of cancer is unclear, a limited number of studies suggest that α-syn might be involved in the regulation of tumor differentiation. Supporting this possibility, α-syn was preferentially expressed in brain tumors showing neuronal differentiation (28). In cell cultures expression of α-syn was increased during the hematopoietic differentiation of K562 myelogenous leukemia cells (31). Similarly, it was shown that α-syn was up-regulated during neural differentiation of pheochromocytoma PC12 cells (32). Thus, distinct from the possible role of γ-syn for tumor metastasis, α-syn might be involved in tumor differentiation.

Accordingly, the main objective of the present study was to determine whether α- and/or β-syn might regulate growth and differentiation of cancer cells. For this purpose, α- and β-syn were stably overexpressed in MG63 human osteosarcoma cells. We found that compared with vector-transfected and β-syn-overexpressing cells, α-syn-overexpressing cells exhibited distinct phenotype of differentiated osteoblastic cells. Mechanistically, α-syn may cause down-regulation of proteasome activity, leading to accelerate cellular differentiation. Further studies revealed that down-regulation of proteasome activity by α-syn was regulated by alteration of various factors, including PKC signaling activities and the autophagy-lysosomal pathway in α-syn-overexpressing cells.

EXPERIMENTAL PROCEDURES

Reagent—Chemical reagents include MG132 and lactacystin (purchased from EMD Biosciences, San Diego, CA), rotenone, 12-myristate 13-acetate (PMA), 4α-phorbol 12,13-didecanoate (4αPDD), leupeptin, chelerythrine chloride, and 3-methyladenine (3-MA) (obtained from Sigma), and caspase I inhibitor and III inhibitors (Ac-AAVALLPAVLLALLAP-YVAD-CHO, Ac-AAVALLPAVLLALLAP-DEVD-CHO) (Calbiochem) were applied to cell cultures at indicated concentrations.

Antibodies used are as follows. Monoclonal antibodies, anti-α-syn (syn-1), anti-β-syn, anti-PKCε, and anti-retinoblastoma (Rb) were purchased from BD Biosciences. Monoclonal anti-β-actin (AC-15) was obtained from Sigma. Monoclonal antibodies anti-p21 and anti-cyclin B1, rabbit polyclonal antibodies anti-p15, anti-cyclin D1, anti-cyclin-dependent kinase 4, and anti-phosphorylated Rb, and goat polyclonal anti-osteocalcin antibody were from Santa Cruz Biotechnology (Santa Cruz, CA). Monoclonal anti-ubiquitin antibody was from Chemicon (Temecula, CA). Monoclonal anti-19 S proteasome S6a subunit antibody was from Biomol (Plymouth Meeting, PA). Rabbit polyclonal anti-cathepsin B was from Calbiochem. Rabbit polyclonal antibodies, anti-C-terminal α-syn, and anti-β-syn were previously described (33, 34). Alexa fluor 488-conjugated anti-goat secondary antibody, Alexa fluor 488-conjugated anti-rabbit secondary antibody, and Alexa fluor 555-conjugated anti-mouse secondary antibody were from Invitrogen.

Cell Cultures and Transfection—MG63 and 293T cells were both cultured in Dulbecco's modified Eagle's medium (high glucose) containing 10% fetal calf serum (BioWest, Nuaille, France) and 1% v/v penicillin/streptomycin (Invitrogen) in a 5% CO_2, 95% air atmosphere. MG63 cells exhibited both α- and β-syn transcripts by RT-PCR analysis, but their protein expressions were hardly detectable by immunoblot analysis (data not shown). For stable transfection, MG63 cells were transfected with pCEP4 expression vector (Invitrogen) or pCEP4 containing either human α- or β-syn cDNA (34) using Lipofectamine 2000 (Invitrogen). After 2~3 weeks of incubation in the presence of 200 μg/ml hygromycin B (EMD Biosciences), the resistant colonies of cells (~20) were isolated. These stable cell lines were routinely maintained in the presence of 50 μg/ml hygromycin B. 293T cells were transiently transfected with p-Target expression vector (Promega, Madison, WI) containing human p21 cDNA insert.[3]

Reverse Transcriptase (RT)-PCR—Total RNA was isolated from cultured cells using the RNA extraction buffer ISOGEN (Nippon Gene, Tokyo, Japan). cDNA was synthesized from 2 μg of total RNA using the Superscript III First-Strand Synthesis system (Invitrogen) according to the manufacturer's instruction.

PCR amplification was carried out using Taq PCR polymerase (ABgene, Tokyo, Japan), and the amplified products were resolved by agarose gel electrophoresis. The following primers were used for PCR. Human α-syn (NM_000345): sense, 5′-ATGGATGTATTCATGAAAGGACTTTC-3′ (47–72-oligonucleotide position), antisense, 5′-GGCTTCAGGTTCGTAGTCTTGATAC-3′ (the 442–466 oligonucleotide position); human β-syn (BT006627): sense, 5′-ATGGACGTGTTCATGAAGGGC-3′ (1–21-oligonucleotide position), antisense, 5′-CTACGCCTCTGGCTCATACTC-3′ (385–405-oligonucleotide position); human cyclophilin A (NM_021130): sense, 5′-TACTATTAG-

[3] T. Urano, unpublished information.

CCATGGTCAAC-3′ (62–81-oligonucleotide position), antisense 5′-GTCTTGCCATTCCTGGACCC-3′ (508–527-oligonucleotide position); human liver/bone/kidney-type alkaline phosphatase (ALP) (AB011406): sense, 5′-GGGGGTGGCCGGAAATACAT-3′ (834–853-oligonucleotide position), antisense, 5′-GGGGGCCAGACCAAAGATAG-3′ (1357–1376-oligonucleotide position); human osteocalcin (X51699): sense, 5′-ATGAGAGCCCTCACACTCCTC-3′ (19–39-oligonucleotide position), antisense, 5′-GCCGTAGAAGCGCCGATAGGC-3′ (292–312-oligonucleotide position).

Immunoblot and Co-immunoprecipitation Analyses—Immunoblot analysis was performed as previously described (34). Briefly, cells were harvested and dissolved in lysis buffer (1% Nonidet P-40, 50 mM HEPES, 150 mM NaCl, 10% glycerol, 1.5 mM $MgCl_2$, 1 mM EGTA, 100 mM sodium fluoride, and protease inhibitor mixture (Nakarai Tesque, Kyoto, Japan)). Protein concentrations of the cell lysates were determined Bio-Rad protein assay reagent. Cell extracts (10 μg) were then resolved by SDS-PAGE (10 or 16%) and electroblotted onto nitrocellulose membranes (GE Healthcare) with CAPS buffer (pH 11.0). The membranes were blocked with 3% bovine serum albumin (BSA) in Tris-buffered saline (TBS: 25 mM Tris-HCl (pH 7.5), 150 mM NaCl) plus 0.2% Tween 20 followed by an incubation with primary antibodies in TBS containing 3% BSA. After washing, the membranes were further incubated with second antibody conjugated with horseradish peroxidase (GE Healthcare) in Tris-buffered saline (1:10,000). Finally, the target proteins were visualized with the ECL plus system (GE Healthcare). The intensity of the band was measured using BioMax 1D image analysis soft ware (Eastman Kodak Co.). In some experiments 293T cells were transfected with p-Target vector (Promega) with or without human p21 cDNA insert, and cell extracts were used for controls. Recombinant human α- and β-syn were also used for positive controls (9).

Immunoprecipitation was performed as previously described (35). Briefly, cell extracts (200 μg) were preabsorbed with protein G-Sepharose (GE Healthcare) for 1 h, and the precleared lysates were incubated with either syn-1 or mouse IgG control (each 1 μg) overnight at 4 °C followed by incubation with protein G-Sepharose. The immune complexes were then washed three times with the lysis buffer. The samples were then heated in the SDS sample buffer for 5 min and subjected to immunoblotting.

Immunofluorescence Study—Cells were seeded onto poly-L-lysine-coated glass coverslips, grown to 70% confluence, fixed in 4% paraformaldehyde for 30 min and pretreated with 0.1% Triton X-100 in phosphate-buffered saline (PBS) for 20 min. Fixed cells were blocked with PBS containing 3% goat serum and 5% bovine serum albumin at room temperature. For staining, cells were incubated overnight at 4 °C with primary antibody (or antibodies for double staining). After washing, cells were incubated with Alexa fluor-conjugated secondary antibody (or antibodies for double staining) (Invitrogen) for 1 h at room temperature. Control experiments included immunostaining in the absence of primary antibody. Coverslips were air-dried, mounted on slides with Gel/Mount (Biomeda Corp., Foster City, CA), and imaged with the laser-scanning confocal microscope (LSCM) (Olympus, FV1000, Tokyo, Japan).

Cell Cycle Analysis Using Flow Cytometry—Cells seeded at 1×10^5 cells in 6-well cell culture plates were incubated under low serum (0.1%) conditions for 24 h, treated with 10% serum for 6, 12, 18, 24, and 96 h, and harvested using trypsin-EDTA. After washing with PBS, cells were fixed by ice-cold ethanol to final concentration of 70%. The cells were then resuspended in PBS containing 0.5 mg/ml RNaseA (Nakarai Tesque), incubated for 30 min at 37 °C, and followed by staining with propidium iodide (10 μg/ml) for 10 min at room temperature. Before flow cytometry analysis, the stained cells were filtrated with nylon mesh. The fluorescence signals of 2×10^4 cells were recorded by EPICS ALTRA (Beckman Coulter, Fullerton, CA). The distribution of cell cycle phase was analyzed by Multicycle software (Phoenix Flow Systems, San Diego, CA).

Measurement of ALP Activity—Cellular activities of ALP were determined as described previously with some modifications (36). Briefly, cells were grown until confluency under the 10% serum conditions in 6-well cell culture plates. Cells were then washed twice, harvested into PBS, and sonicated by ultrasonic disruptor (TOMY, Tokyo, Japan) for 20 s. After centrifugation of the cell preparations at 15,000 rpm for 10 min, the supernatants were recovered and assessed for protein concentration. The supernatants (10 μg) were then incubated in the ALP assay buffer containing 10 mM *p*-nitrophenyl phosphate (Sigma), 100 mM glycine, 1 mM $ZnCl_2$, and 1 mM $MgCl_2$ (pH 10.4). After 90 min of incubation at 37 °C, ALP activity was determined by monitoring the amount of released *p*-nitrophenol at 415 nm. Dissolved *p*-nitrophenol in assay buffer was used to establish the standard for quantification. The released *p*-nitrophenol was adjusted by the amount of protein and described as nmol/min/mg of protein.

Increased levels of the cellular ALP activities were further confirmed by direct stain of the cells. The cells reached confluency were fixed with 70% ethanol, washed twice with Tris-buffered saline, and incubated with nitro blue tetrazolium chloride/5-bromo-4-chloro-3-indolyl phosphate *p*-toluidine salt ALP substrate solution (Roche Applied Science) for 2 h. The visualized image was then photographed.

Mineralization Assay—Mineralization of MG63 cells was performed as previously described (36) with some modifications. Briefly, cells were grown until confluency under the 10% serum conditions in 24-well cell culture plates. The cells were further incubated in α-minimal essential medium (Invitrogen) plus 10% serum in the presence of 10 mM β-glycerophosphate (Sigma) and 50 μg/ml ascorbic acid with or without the addition of various chemical reagents. The media were regularly changed twice a week. After 4 weeks, cells were evaluated for the extent of matrix mineralization by either alizarin red staining or von Kossa staining. For alizarin red staining, the cells were fixed with 70% ethanol for 30 min at room temperature. Then the cells were incubated with 40 mM alizarin red-S (Sigma) for 10 min and washed 4 times with distilled water. The visualized image was photographed. For von Kossa staining, the cells were fixed with 10% neutralized formaldehyde for 30 min at room temperature. The fixed cells were incubated with 5% silver nitrate for 5 min under the exposure to the sunlight. The reaction was stopped by the addition of 5% sodium thiosulfate.

The stained cells were washed four times with distilled water and imaged with microscope.

Evaluation of Proteasome and Cathepsin B Activity—Measurement of proteasome and cathepsin B activity was done as previously described with modifications (37). Briefly, cells reaching confluency in 6-well cell culture plates were incubated under the low serum (0.1%) conditions for 24 h and treated with 10% serum with or without treatment of various reagents. After the indicated times (0, 6, or 12 h), the cells were harvested in buffer containing 50 mM HEPES (pH 7.4), 10 mM EDTA, and 10 mM NaCl, subjected to freezing and thawing to rapture cell membranous structures, and then centrifuged at 15,000 rpm for 10 min. For the measurement of proteasome activity, 10 μg of the supernatants were incubated in assay buffer containing 50 mM HEPES (pH 7.4), 10 mM EDTA, 10 mM NaCl, and 40 μM benzyloxycarbonyl-Leu-Leu-Glu-amidomethylcoumarin fluorogenic proteasome substrate (Chemicon). For cathepsin B activity, 10 μg of the supernatants were incubated in buffer containing 50 mM HEPES (pH 6.0), 10 mM EDTA, 10 mM NaCl, and 40 μM benzyloxycarbonyl-Arg-Arg-amidomethylcoumarin fluorogenic cathepsin B substrate (Chemicon). These enzyme activities were assayed by continuous recording of the fluorescence activity released from fluorogenic substrate using Berthold Mithras LB940 microplate reader (Berthold, Bad Wildbad, Germany) for 1 h at 37 °C (excitation, 380 nm; emission, 460 nm), and the reaction rate was analyzed. These enzyme activities were described as arbitrary unit/min/mg of protein.

Evaluation of PKC Activity—PKC activity was determined using PepTag nonradioactive PKC assay kit (Promega) according to the manufacture's instruction. Briefly, cells reaching confluency in 6-well cell culture plates were treated with or without PMA for 20 min and harvested in extraction buffer (25 mM Tris-HCl (pH 7.4), 0.5 mM EDTA, 0.5 mM EGTA, 10 mM β-mercaptoethanol, 100 mM phenylmethylsulfonyl fluoride, and protease inhibitor mixture (Nakarai Tesque)). Cell extracts were then sonicated by ultrasonic disruptor (TOMY) for 20 s and centrifuged at 15,000 rpm for 15 min. The supernatants were used for the assay. The reaction was performed at 30 °C for 30 min in assay solution including, PepTag C1 peptide (0.4 μg/μl) and 5 μg of protein sample. The samples were separated on the 0.8% agarose gel and visualized on a transilluminator. The intensity of fluorescence of the phosphorylated peptides were quantified using BioMax 1D image analysis soft ware (Kodak).

Electron Microscopy—Electron microscopy analysis was performed as previously described with minor modifications (38). Briefly, cells were harvested using trypsin-EDTA and fixed by 2.5% glutaraldehyde in 0.1 M sodium cacodylate buffer at 4 °C for 2 h. After centrifugation, cells were washed with 0.1 M sodium cacodylate buffer 3 times. Cell pellets were obtained by centrifuge, post-fixed in 1% osmium tetroxide and 1% potassium ferrocyanide at room temperature for 2 h, and processed for embedding in Quetol 812 (Nisshin EM, Tokyo, Japan). Ultrathin sections were stained with uranyl acetate and lead nitrate and observed by a Hitachi H-7500 electron microscope.

Statistical Analysis—All values in the figures are expressed as means ± S.D. To determine statistical significance, the values were compared by two group *t* tests. The differences were considered as significant if *p* values were less than 0.05.

RESULTS

Overexpression of Syn in MG63 Osteosarcoma Cells—To investigate the effect of syn on growth and differentiation of tumor cells, MG63 osteosarcoma cells were stably transfected with α- or β-syn cDNA. Three high expressors of α-syn (clones α1, α5, and α15) and β-syn (clones β5, β8, and β13) were selected on the basis of immunoblot analysis together with empty vector-transfected cells (clones v2, v5, and v10) (Fig. 1*A*). For the majority of experiments, clone α1, the high expresser of α-syn, and clones β5 and v2 were used. Immunoblot analysis also showed that the immunoreactivities of both α- and β-syn were almost exclusively those of their monomers (Fig. 1*A*). To further analyze expression and distribution of syn proteins, double immunolabeling/LSCM was performed using at least two antibodies for each syn (Fig. 1*B*). The immunoreactivity of α-syn in α-syn-overexpressing cells (α1) was diffuse in the cell bodies as detected by both monoclonal syn-1 and polyclonal C-terminal antibodies (*a* and *b*). Immunoreactivity of β-syn in β-syn-overexpressing cells (β5) was also localized diffusely in the cell bodies by monoclonal anti-β-syn antibody (*e*) but was detected with a shift to perinuclear regions by polyclonal anti-β-syn antibody (*f*). In none of these cases, inclusion bodies were detected. Notably, expression levels of α-syn were heterogeneous (*c*), and similar patterns were consistently observed in all the three clones of α-syn-overexpressing cells (data not shown). By contrast, immunoreactivities of β-syn were homogeneous in β-syn-overexpressing cells (*g*). No immunoreactivities of syn proteins were detected in vector-transfected cells (v2) (*d* and *h*).

To determine whether cell proliferation was affected by overexpression of syn, the stable clones were evaluated for their cell growth rates. The doubling times of cells in log phase of growth under 10% serum conditions were 20–24 h for α-syn-overexpressing cells and 14–17.5 h for both β-syn-overexpressing and vector-transfected cells (data not shown). Cells were then incubated under the low serum (0.1%) for 24 h to synchronize at G_1 in cell cycle and then added with 10% serum followed by counting of cell numbers at the indicated times. The result showed that that the average cell numbers of α-syn-overexpressing cells at day 4 were significantly decreased compared with both β-syn-overexpressing and vector-transfected cells (Fig. 1*C*).

To determine whether decreased cell proliferation of α-syn-overexpressing cells is due to alteration of cell cycle profile, cell cycle analysis was performed using flow cytometry at varying time periods (0, 6, 12, 18, 24, and 96 h) after the addition of 10% serum to serum-deprived cells. The result showed that compared with both β-syn-overexpressing and vector-transfected cells, α-syn cells in G_0/G_1 phases were significantly increased ($p < 0.05$), whereas those in both S and G_2/M phase were decreased at 24 and 96 h ($p < 0.05$) (Fig. 1*D*). Essentially similar results were observed at 96 h. However, compared with the profile at 24 h, there were more cells in G_0/G_1 phase, fewer cells in S phase, and more cells in G_2/M at 96 h. One possible reason for the difference between 24 and 96 h could be that at 24 h many cells might have not yet reached G_2/M phase. Furthermore, a relatively high ratio of cells in G_0/G_1 phase at 96 h could

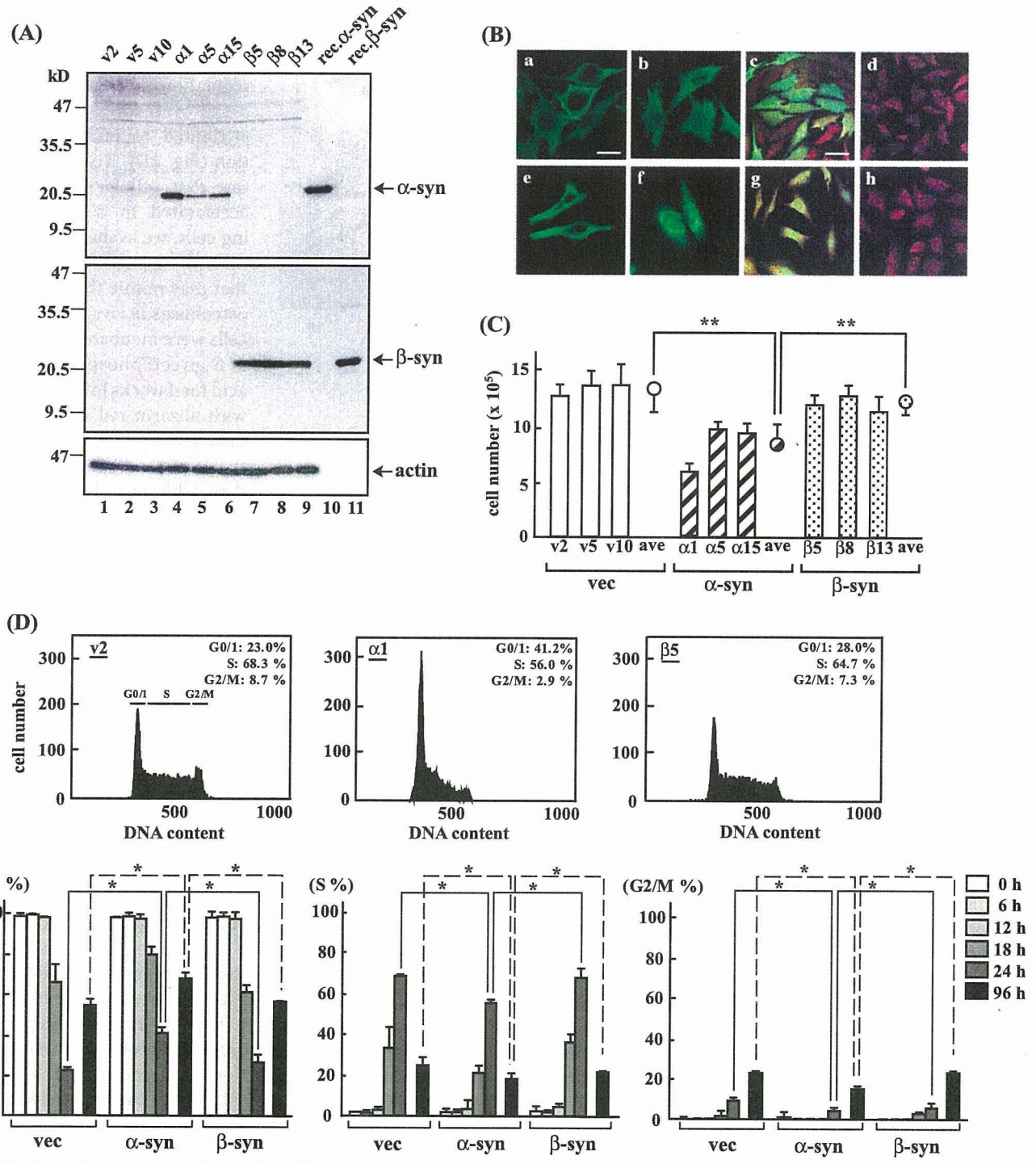

FIGURE 1. **Analysis of syn expression in transfected MG63 osteosarcoma cells.** *A*, immunoblot analysis of syn proteins. Cell extracts were analyzed by immunoblotting using syn-1 (*upper panel*), anti-β-syn monoclonal antibody (*middle panel*), and anti-actin antibody (*lower panel*). Three vector-transfected clones (v2, v5, v10, *lanes 1–3*), three high expresser clones for α-syn (α1, α5, α15, *lanes 4–6*), and β-syn (β5, β8, β13, *lanes 7–9*) are shown. Recombinant α- and β-syn proteins were used as positive controls (*lanes 10* and *11*). *B*, immunofluorescence/LSCM analysis of syn expression. α-Syn-overexpressing cells (α1) (*a–c*), β-syn-overexpressing cells (β5) (*e–g*), and vector-transfected cells (v2) (*d* and *h*) were immunostained with antibodies against α-syn (*green*, *a–d*), β-syn (*green*, *e–h*), and actin (*red*, *c*, *d*, *g*, and *h*) followed by observation by LSCM. α-Syn was diffusely distributed in the cell bodies with a slight shift to cell membrane as detected by both syn-1 (*a*) and polyclonal c-terminal antibody (*b*). β-Syn was similarly detected in the cell bodies by monoclonal anti-β-syn antibody (*e*), but strong stains of perinuclear regions were observed by polyclonal anti-β-syn antibody (*f*). Immunoreactivities of α-syn were heterogeneous (*c*), whereas those of β-syn were almost even in all cell populations (*g*). No immunoreactivities of syn proteins were detected in vector-transfected cells (*d* and *h*). *Bars* represent either 20 μm for high magnification (*a*, *b*, *e*, and *f*) or 50 μm for low magnification (*c*, *d*, *g*, and *h*). *C*, evaluation of cell proliferation. Cells (v2, v5, v10, α1, α5, α15, β5, β8, and β13) were incubated at 1×10^5 cells/well in the 6-well plates under the low serum (0.1%) conditions for 24 h to synchronize. Cells were then treated with 10% serum, and cell numbers were counted at 96 h. *Open circles* represent the group mean values. Data shown are the mean ± S.D. ($n = 3$). **, $p < 0.01$. *D*, flow cytometry for cell cycle analysis. Cells were prepared as described in *C*, and DNA contents were analyzed at the indicated times (0, 6, 12, 18, 24, and 96 h) after serum stimulation. The *upper figures* are a typical cell cycle profile at 24 h for v2, α1, and β5. The *x* axis represents the fluorescent intensities proportional to the amount of DNA, whereas the *y* axis indicates the cell number. The *lower column figures* show that G_0/G_1 phases at 24 and 96 h in α-syn cells were significantly increased, whereas those in both S and G_2/M phase were decreased compared with both β-syn-overexpressing and vector-transfected cells. Data presented are the mean ± S.D. of triple determinations. *, $p < 0.05$.

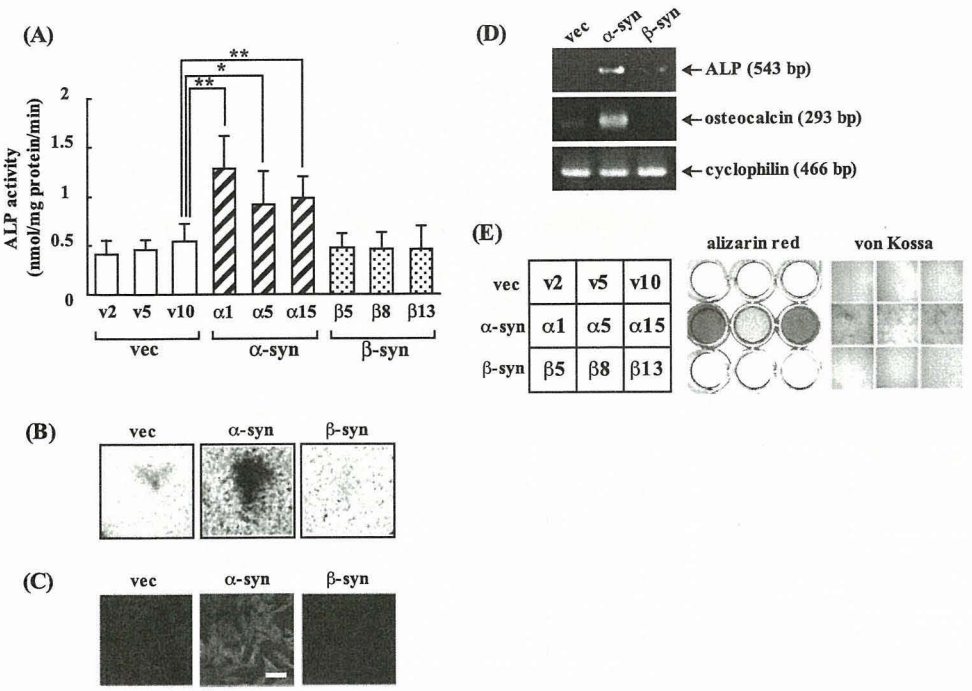

FIGURE 2. **Up-regulation of the expression of osteoblastic differentiation markers in α-syn-overexpressing MG63 cells.** *A*, measurement of ALP activity. Cells (v2, v5, v10, α1, α5, α15, β5, β8, and β13) under the confluent conditions were harvested, and cell extracts were incubated with *p*-nitrophenyl phosphate at 37 °C for 90 min. The amount of released nitrophenol was monitored by absorbance at 415 nm. α-Syn-overexpressing cells (α1) showed significantly higher ALP activity compared with other cell types (v2 and β5). Data shown are mean ± S.D. ($n = 5$). *, $p < 0.05$; **, $p < 0.01$. *B*, evaluation of ALP activity by staining. Cells (v2, α1, and β5) were stained with nitro blue tetrazolium chloride/5-bromo-4-chloro-3-indolyl phosphate solution and photographed. *C*, immunostaining of osteocalsin. Cells (v2, α1, and β5) were immunostained with anti-osteocalsin antibody followed by observation with LSCM. The *bar* represents 50 μm. *D*, RT-PCR analysis of ALP and osteocalcin mRNAs. Cyclophilin mRNA was used as an internal control. *E*, *in vitro* mineralization assay. Cells (v2, v5, v10, α1, α5, α15, β5, β8, and β13) were seeded onto 24-well cell culture plates (1×10^5 cells/ml) and maintained in α-minimal essential medium containing 10 mM β-glycerophosphate and 50 μg/ml ascorbic acid for 4 weeks. Matrix mineralization was evaluated by either alizarin red staining (*middle panel*) or von Kossa staining (*right panel*). Each clone number is indicated in the squire matrix (*left panel*). Please note that the strongest staining was observed in clone α1, the highest α-syn expresser.

be due to the decreased nutrients in the culture medium after long time culture. Taken together, these results suggested that overexpression of α-syn, but not of β-syn, suppressed cell proliferation in MG63 osteosarcoma cells.

α-Syn-overexpressing MG63 Cells Exhibit Enhanced Differentiation Phenotype—Based on the apparent decrease of growth rates and enhanced G_0/G_1 phases in cell cycle in α-syn-overexpressing MG63 cells compared with β-syn-overexpressing and vector-transfected cells, we speculated that the former cells might be shifted to cellular differentiation.

To test this possibility, we evaluated ALP since this molecule had been widely used as a marker for osteoblastic differentiation. As we suspected, all three clones of α-syn-overexpressing cells displayed significantly higher activity of ALP compared with both β-syn-overexpressing and vector-transfected cells (Fig. 2*A*). Activation of ALP was also assessed by direct stain of cells using nitro blue tetrazolium chloride/5-bromo-4-chloro-3-indolyl phosphate as substrate. The result showed that the intensity of the staining in α-syn-overexpressing cells was much stronger than those of β-syn-overexpressing and vector-transfected cells (Fig. 2*B*). Next, we analyzed expression of osteocalcin, another marker for osteoblastic differentiation. The immunofluorescence/LSCM study showed that immunoreactivity of osteocalcin was strongly observed in α-syn-overexpressing cells but not in other cell types (Fig. 2*C*). Furthermore, RT-PCR analysis revealed that up-regulation of ALP and osteocalcin in α-syn-overexpressed cells might be attributed to increased transcription (Fig. 2*D*). To further corroborate that cellular differentiation is accelerated in α-syn-overexpressing cells, we evaluated formation of mineral deposition in the matrix that may mimic the calcification by osteoblasts *in vivo*. For this purpose, cells were incubated in the presence of β-glycerophosphate and ascorbic acid for 4 weeks followed by staining with alizarin red to assess calcium incorporation. The result showed that mineralization was clearly detectable in α-syn-overexpressing cells but not in β-syn-overexpressing nor vector-transfected cells (Fig. 2*E*). Similar results were obtained by von Kossa staining for the assessment of bone nodule formation (Fig. 2*E*). Taken together, α-syn-overexpressing cells specifically exhibited a differentiated phenotype compared with both β-syn-overexpressing and vector-transfected cells.

Alteration of G_1 Cell Cycle Regulators and Decreased Proteasome Activity in α-Syn-overexpressing MG63 Cells—Because prolonged G_1 period in cell cycle is prerequisite for cell entry into G_0 and further differentiation, it was predicted that expressions and activities of various G_1 cell cycle regulators might be altered in α-syn-overexpressing cells.

To test this possibility, cells were incubated under the low serum (0.1%) conditions for 24 h to synchronize at G_1 followed by 10% serum treatment. Cells were then harvested, and expression of various cell cycle regulators were analyzed at the indicated times (Fig. 3*A*). Notably, expression of the cyclin-dependent kinase inhibitor p21, one of the key molecules which negatively regulate cell cycle progression from G_1 to S phase, was significantly up-regulated in α-syn-overexpressing cells. In these cells p21 was constitutively expressed without serum stimulation and was further increased in response to serum, reaching the maximum around 6- 12 h followed by gradual decrease. By contrast, in vector-transfected cells expression of p21 was transiently up-regulated at 6 h and immediately decreased. Consistent with this, phosphorylation of Rb protein was compromised in α-syn-expressing cells compared with vector-transfected cells. Furthermore, cyclin B1, a marker for G_2/M phase, was up-regulated earlier in vector-transfected cells than in α-syn-overexpressing cells. As for other cyclin-dependent kinase inhibitors, p15 level was slightly elevated at 24- and 48-h time points, whereas expression of p27 was not up-

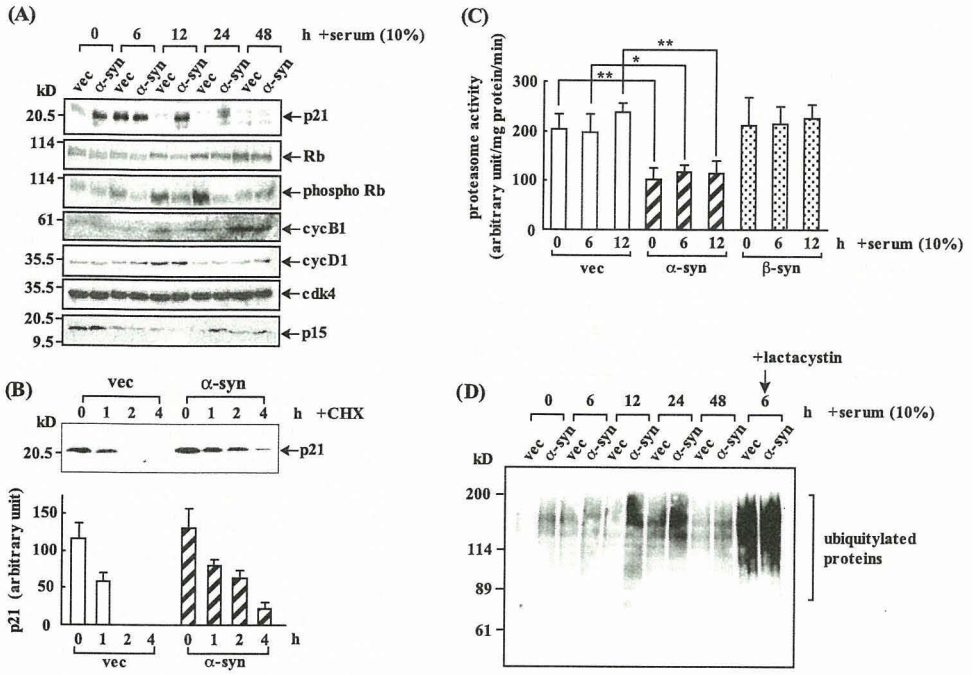

FIGURE 3. **Altered expression of cell cycle regulators and decrease of proteasome activity in α-syn-overexpressing MG63 cells.** *A*, immunoblot analysis of cell cycle regulators. Vector-transfected (v2) and α-syn-overexpressing cells (α1) were incubated under the low serum (0.1%) conditions for 24 h to synchronize and then treated with 10% serum for the indicated times (6, 12, 24, and 48 h). Cells were then harvested, and cell lysates were analyzed by immunoblotting with anti-p21, Rb, phospho Rb, cyclin (*cyc*) B, cyclin D1, cyclin-dependent kinase (*Cdk4*), p15, and ubiquitin. *B*, evaluation of the stability of p21 protein by cycloheximide experiments. The synchronized cells (v2 and α1) were treated with 10% serum with or without cycloheximide (*CHX*) for the indicated times (1, 2, and 4 h), and cell lysates were analyzed by immunoblotting (*upper panel*). Each band was quantified using BioMax 1D image analysis soft ware (*lower panel*). Data shown are the mean ± S.D. Similar results were obtained by three independent experiments. *C*, measurement of proteasome activity. Cells (v2, α1, and β5) were incubated under the low serum (0.1%) conditions for 24 h and then treated with 10% serum for the indicated times (6 and 12 h). To evaluate proteasome activity, cell extracts (10 μg) were incubated with fluorogenic substrate (benzyloxycarbonyl-Leu-Leu-Glu-amidomethylcoumarin) at 37 °C. Released fluorescence (excitation 380 nm, emission 460 nm) was monitored by 5 min intervals up to 60 min. The fluorogenic value at each time point was plotted, and the slope was calculated. Data shown are the mean ± S.D. ($n = 3$). *, $p < 0.05$; **, $p < 0.01$. *D*, immunoblot analysis of ubiquitylated proteins. Vector-transfected (v2) and α-syn-overexpressing cells (α1) were prepared as described in *A* and analyzed by immunoblotting using anti-ubiquitin antibody. Both types of cells treated with lactacystin for 6 h were included as positive controls.

regulated in α-syn-overexpressing cells compared with vector-transfected cells (Fig. 3*A* and data not shown). Expression of other cell cycle regulators such as cyclin D1 and cyclin-dependent kinase 4 were not much different between both cell types. Similar expression patterns of p21 and phosphorylated Rb were observed between β-syn-overexpressing cells and vector-transfected cells (data not shown).

Next, to determine whether up-regulation of p21 expression was due to the stabilization of p21 protein in α-syn-overexpressing cells, these cells were treated with cycloheximide to inhibit protein synthesis 6 h after serum stimulation. Under these conditions, expression levels of p21 protein quickly decreased within 2 h of treatment in vector-transfected cells, whereas expression levels in α-syn-overexpressing cells took longer to detect (Fig. 3*B*). Under the same experimental conditions, p21 mRNA was evaluated by real time PCR. However, no significant differences were observed between α-syn-overexpressing and vector-transfected cells (data not shown).

To further determine whether increased stability of p21 was due to compromised degradation by UPS in α-syn-overexpressing cells, syn-transfected cells were analyzed for proteasome activities. The result showed that the proteasome activities of α-syn-overexpressing cells were decreased to ~50% of those of vector-transfected cells, whereas those of β-syn-overexpressing cells were little affected (Fig. 3*C*). Under the same experimental conditions, immunoreactivities of polyubiquitylated proteins were significantly stronger in α-syn-overexpressing cells compared with those in vector-transfected and β-syn-overexpressing cells (Fig. 3*D* and data not shown). Taken together, expression of cell cycle regulators such as p21 and phosphorylated Rb were altered in α-syn-overexpressing cells, which might be attributed to the decreased proteasome activity.

Proteasome Inhibitors Stimulate Differentiation of Wild-type MG63 Cells—If suppression of proteasome activity by α-syn plays a causative role for stimulation of differentiation in MG63 osteosarcoma cells, then it is possible that down-regulation of proteasome activity by other experimental procedures might similarly stimulate differentiation in these cells.

To test this possibility, wild-type MG63 cells were treated with proteasome inhibitors, including MG132 and lactacystin followed by evaluation of cellular differentiation. Immunoblot analysis revealed that administration of these reagents at 10 μM clearly up-regulated p21 expression at 12 h (Fig. 4*A*). Under the same experimental conditions, ALP activity was significantly up-regulated, and immunoreactivity of osteocalcin became detectable (Fig. 4*B* and data not shown). In addition, the expression of ALP and osteocalcin mRNA was up-regulated in lactacystin-treated cells (Fig. 4*C*). Furthermore, cells were induced to form matrix mineralization with lower concentrations of proteasome inhibitors (0.01–0.1 μM for MG132 and 0.1–1.0 μM for lactacystin) in long-term cultures. High concentration (10 μM) treatment of these reagents caused prominent cell death within 48 h (data not shown). By contrast, sublethal concentrations (0.01–0.1 μM) of rotenone, an inhibitor of mitochondria complex I, caspase I, and III inhibitors (0.1–1.0 μM), and leupeptin (1–10 μM) had little effect on cellular differentiation (Fig. 4*D*). Taken together, treatment of wild-type MG63 cells with proteasome inhibitors resulted in stimulation of cellular differentiation.

Down-regulation of PKC Activity in α-Syn-overexpressing MG63 Cells—Our hypothesis was that alteration of signal transduction might be involved in the suppression of proteasome activity in α-syn-overexpressing cells. In this regard we especially focused on the potential role of PKC since it was recently shown that treatment of skeletal muscle by phorbol

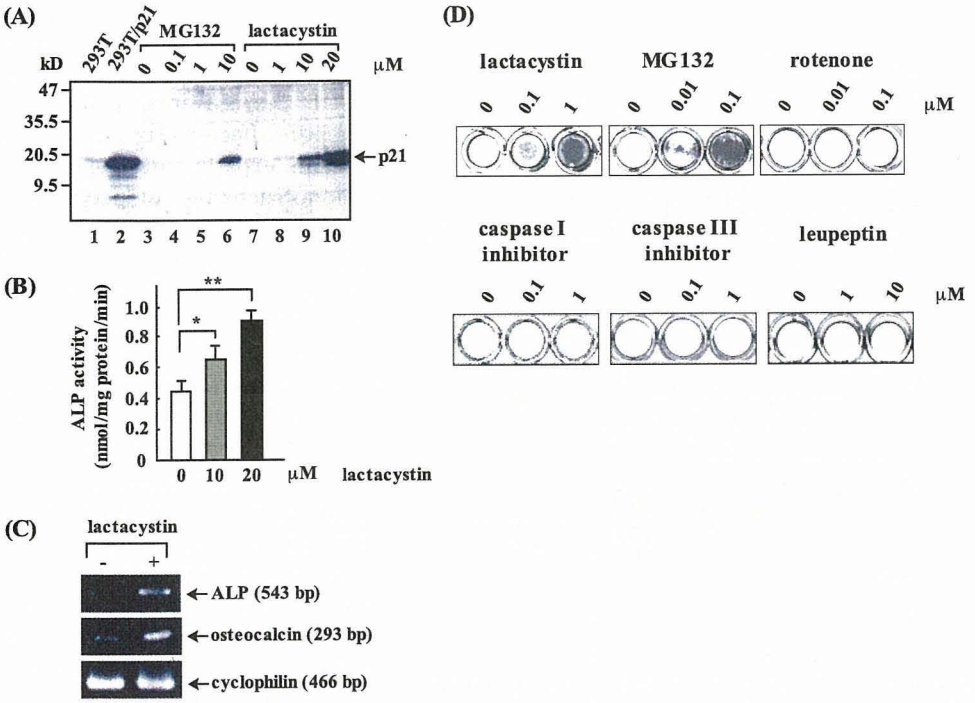

FIGURE 4. **Proteasome inhibitors induce cellular differentiation in wild-type MG63 cells.** Wild-type MG63 were incubated under the low serum (0.1%) conditions for 24 h and then treated with 10% serum in the presence of either MG132 or lactacystin. *A*, immunoblot analysis of p21. Cells were treated with various concentrations of either MG132 (0, 0.1, 1.0, 10 μM, *lanes 3–6*) or lactacystin (0, 1.0, 10, 20 μM, *lanes 7–10*) and harvested at 12 h. Cell lysates were analyzed by immunoblotting using anti-p21 antibody. Extracts of 293T cells transfected with or without p21 expression vector are shown as controls (*lanes 1* and *2*). *B*, measurement of ALP activity. Cells were treated with various concentrations (0, 10, 20 μM) of lactacystin for 12 h. To evaluate ALP activity, cell extracts were incubated with *p*-nitrophenyl phosphate at 37 °C for 90 min. The amount of released nitrophenol was monitored by the absorbance at 415 nm. Data shown in the *left panel* are the mean ± S.D. ($n = 3$). *, $p < 0.05$; **, $p < 0.01$. *C*, RT-PCR analysis of ALP and osteocalcin mRNAs. Cells were treated with lactacystin (10 μM) for 24 h. Cyclophilin mRNA was used as an internal control. *D*, *in vitro* mineralization assay. Cells were treated with various reagents, including MG132 (0, 0.01, 0.1 μM), lactacystin (0, 0.1, 1.0 μM), rotenone (0, 0.1, 0.1 μM), caspase I inhibitor (0, 0.1, 1.0 μM), caspase III inhibitor (0, 0.1, 1.0 μM), and leupeptin (0, 1, 10 μM) for 4 weeks. Matrix mineralization was evaluated by alizarin red staining. Please note that positive staining was observed for cells treated with proteasome inhibitors. Acridine orange/ethidium bromide staining revealed that cells were alive during mineralization (not shown).

ester resulted in stimulation of proteasome activity (39) and it was previously shown that α-syn bound with PKC and down-regulated the activity of PKC in α-syn overexpressing neuroblastoma cells (40).

To determine whether α-syn associates with PKC, a co-immunoprecipitation experiment was performed (Fig. 5*A*). Cell extracts of α-syn-overexpressing cells were immunoprecipitated with syn-1 followed by immunoblotting analysis with mouse anti- PKCε antibody. In agreement with a previous study by Ostrerova *et al.* (40), the result showed that PKCε was specifically co-immunoprecipitated with α-syn.

Next, to further determine whether α-syn colocalize with PKC, cells were double-immunolabeled with anti-α-syn rabbit polyclonal antibody and anti-PKCε antibody followed by observation with LSCM. As shown in Fig. 5*B*, immunoreactivities of α-syn and PKCε considerably overlapped in the cytoplasm of α-syn-overexpressing cells. We observed that PKCε and PKCλ were highly expressed in addition to moderate expression of other PKC family of peptides in MG63 cells (data not shown). Similar results were obtained by both co-immunoprecipitation and double immunolabeling/LSCM studies for PKCλ (data not shown).

Finally, to determine whether PKC activity was compromised in α-syn-overexpressing cells, the syn-transfected cells were treated with or without PMA and analyzed for their PKC activities (Fig. 5*C*). The result showed that proteasome activities of α-syn-overexpressing cells were significantly lower than those of β-syn-overexpressing and vector-transfected cells. Importantly, PMA treatment of α-syn-overexpressing cells restored the PKC activity to the basal levels of those in other cell types. Taken together, these results suggested that α-syn might directly suppress the PKC activity in α-syn-overexpressing cells.

Because previous studies suggested an alternative possibility that α-syn bound with S6 subunit of 19 S proteasome, leading to interference with proteasome functions (41–43), we investigated the association of α-syn with S6a. The results of co-immunoprecipitation experiment confirmed the association of these molecules (Fig. 5*A*). Double immunolabeling/LSCM showed that overlapping of the immunoreactivities of these molecules was partially detected in the cell bodies, since S6a was considerably localized in the nucleus (Fig. 5*B*).

Phorbol Ester Treatment of α-Syn-overexpressing MG63 Cells Restores Proteasome Activity and Suppresses Cellular Differentiation—If suppression of PKC activity by α-syn is causative for down-regulation of proteasome activity and enhanced differentiation in α-syn-overexpressing cells, then stimulation of PKC might restore the proteasome activity and abrogate cellular differentiation in these cells.

Accordingly, α-syn-overexpressing cells were treated with phorbol ester followed by evaluation of proteasome activity. The results showed that the compromised activity of proteasome in α-syn-overexpressing cells was significantly improved by treatment with PMA both at 10 and 50 nM but not with an inactive analogue 4αPDD (Fig. 6*A*). On the other hand, although proteasome activity of vector-transfected cells was increased by treatment with 50 nM PMA, there were little effects observed at 10 nM PMA (Fig. 6*A*). Thus, α-syn-overexpressing cells responded more sensitively to PMA treatment, suggesting the effect of PMA on proteasome was more specific for α-syn-overexpressing cells, which showed decreased proteasome activity. The stimulatory effects of PMA on the proteasome activity in α-syn-overexpressing cells reached the maximum at 50 nM (data not shown) and were completely abro-

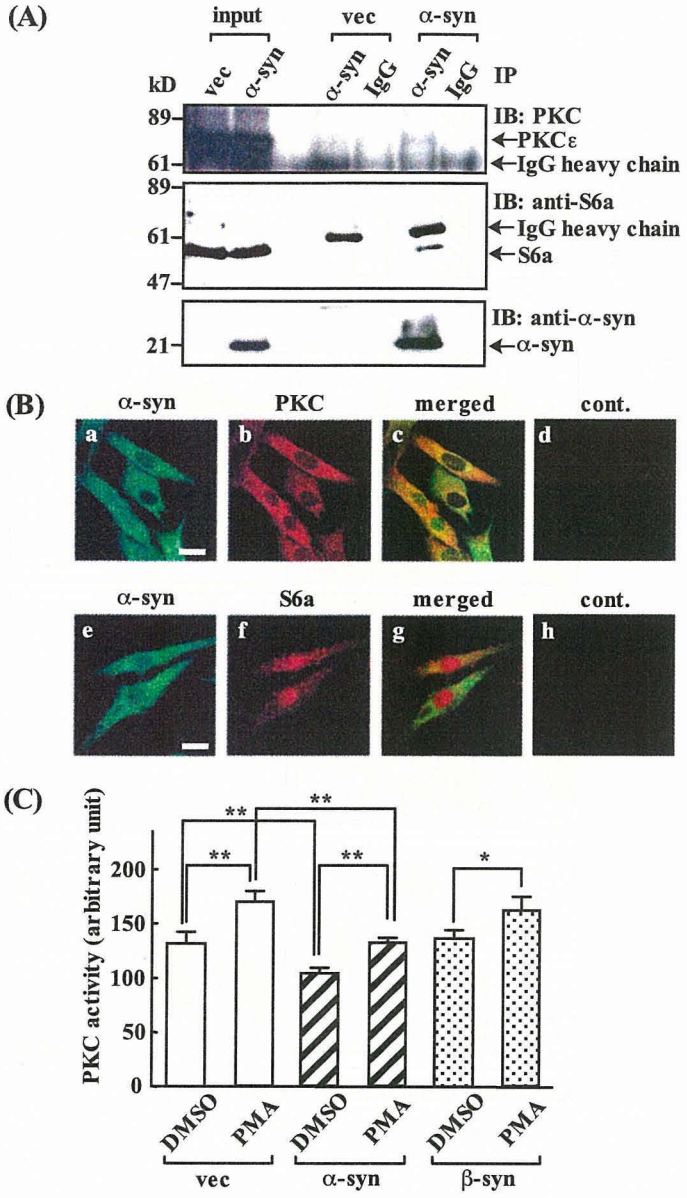

FIGURE 5. **Association of α-syn with PKC and down-regulation of PKC activity in α-syn-overexpressing MG63 cells.** *A*, coimmunoprecipitation (*IP*) of α-syn with either PKCε (*upper*) or S6a (*middle*). Vector-transfected (v2) and α-syn-overexpressing cells (α1) were harvested, and cell extracts (300 μg) were immunoprecipitated with anti-α-syn antibody or mouse IgG control followed by immunoblotting (*IB*)with either anti-PKCε (*upper*), anti-S6a (*middle*), or syn-1 (*low*). Cell extracts (5% of input) were used as positive controls. *B*, immunofluorescence/LSCM of α-syn association with either PKCε or S6a in α-syn-overexpressing cells. Cells (α1) were doubly stained with anti-α-syn antibody (*green*) and either anti-PKCε or S6a (*red*) and observed by LSCM. Please note that α-syn (*red*) and PKCε (*green*) were well co-localized in the cell bodies (*c*). *Bars* represent 50 μm. *C*, measurement of PKC activity. Exponentially growing cells (v2, α1, and β5) were treated with or without PMA for 20 min, and cell extracts (10 μg) were analyzed for PKC activity using fluorogenic peptides as substrates as described under "Experimental Procedures." Data shown are the mean ± S.D. ($n = 3$). *, $p < 0.05$; **, $p < 0.01$. *DMSO*, dimethyl sulfoxide.

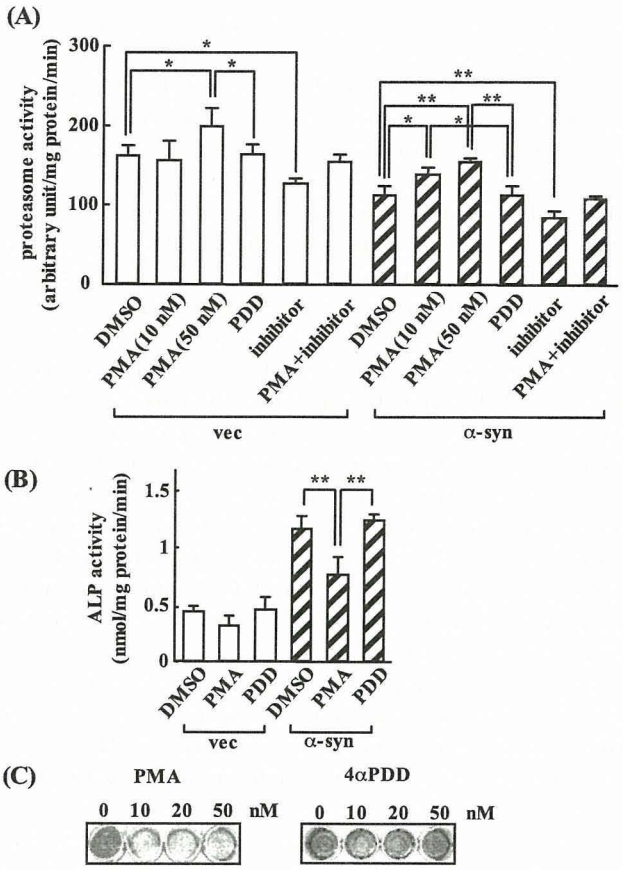

FIGURE 6. **Phorbol ester treatment restores proteasome activity and abrogates differentiation in α-syn-overexpressing MG63 cells.** *A*, measurement of proteasome activity. Vector-transfected (v2) and α-syn-overexpressing cells (α1) were incubated under the low serum (0.1%) conditions for 24 h and then treated with 10% serum in the presence of any of vehicle (0.1% Me_2SO (*DMSO*)), PMA (10 and 50 nM), 4αPDD (50 nM), chelerythrine chloride (PKC inhibitor, 50 nM), or PMA (50 nM) plus chelerythrine chloride (50 nM). Cell extracts (5 μg) were harvested at 12 h after treatment and incubated with fluorogenic proteasome substrate at 37 °C. Released fluorescence (excitation, 380 nm; emission, 460 nm) was monitored each 5 min up to 60 min. Fluorogenic intensity of each time point was plotted, and the slope was calculated. Data shown are the mean ± S.D. ($n = 3$). **, $p < 0.01$. *B*, measurement of ALP activity. Vector-transfected (v2) and α-syn-overexpressing cells (α1) were treated as described in *A*. Cell extracts at 12 h treatment were incubated with *p*-nitrophenyl phosphate at 37 °C for 90 min. The amount of released nitrophenol was monitored by the absorbance at 415 nm. Data shown are the mean ± S.D. ($n = 3$). *, $p < 0.05$; **, $p < 0.01$. *C*, *in vitro* mineralization assay. α-Syn-overexpressing cells (α1) were treated with either PMA or 4αPDD at the indicated concentrations (0, 10, 20, 50 nM). Matrix mineralization was then evaluated by alizarin red staining. Please note that the staining was mitigated by PMA but not by 4αPDD. Similar results were obtained by three independent experiments.

gated in the presence of PKC inhibitor, chelerythrine chloride (Fig. 6*A*), implying that PMA stimulated proteasome activity through phosphorylation but not through depletion of PKC.

Next, to determine whether PKC stimulation of proteasome activity modifies differentiation in α-syn-overexpressing cells, cellular differentiation markers were analyzed. Compared with treatment with either vehicle or inactive 4αPDD, PMA efficiently reduced ALP activity in α-syn-overexpressing cells (Fig. 6*B*). Immunoreactivity of osteocalcin was also decreased by PMA but not by 4αPDD in these cells (data not shown). Finally, it was confirmed that PMA, but not 4αPDD, significantly reduced matrix mineralization in α-syn-overexpressing cells as demonstrated by decreased stains of alizarin red (Fig. 6*C*). Taken together, PMA treatment of α-syn-overexpressing cells restored proteasome activity and abrogation of cellular differentiation in these cells.

Up-regulation of Lysosomal Activity in α-Syn-overexpressing MG63 Cells—Because a recent study has shown that autophagy-lysosomal pathway may play an important role for aggre-

gate-prone proteins, including α-syn and Huntingtin (44), it is reasonable to speculate that down-regulation of proteasome activity by α-syn might be further modulated by this pathway.

In this context we wondered if lysosomal activity might be altered due to increased level of α-syn expression in α-syn-overexpressing cells. To test this hypothesis, cysteine protease cathepsin B, one of the major protease in lysosome, was evaluated. The results showed that cathepsin B was significantly up-regulated in α-syn-overexpressing cells compared with vector-transfected and β-syn-overexpressing cells (Fig. 7*A*). Consistent with this, expression of cathepsin B was up-regulated at protein and mRNA levels in α-syn-overexpressing cells (Fig. 7*B*, data not shown). To investigate the ultrastructure of lysosome, an electron microscopic study was performed. The results revealed extensive lysosomal pathology, such as autolysosome and myelinosome, in α-syn-overexpressing cells (Fig. 7*C*, *a*, *c*, *e*, and *f*). On the contrary, fewer lysosomes were observed in vector-transfected and β-syn-overexpressing cells (Fig. 7*C*, *b* and *d*). Taken together, these results suggested that lysosomal activity was up-regulated in α-syn-overexpressing cells.

Autophagy-lysosomal Inhibitor Treatment Results in Down-regulation of Proteasome Activity, Leading to Acceleration of Cellular Differentiation in α-Syn-overexpressing MG63 Cells—If up-regulation of lysosomal activity in α-syn-overexpressing cells may reflect the compensatory mechanism against the increased level of α-syn, then suppression of autophagy-lysosomal pathways may result in compromised clearance of α-syn, leading to decrease proteasome activity and accelerate cellular differentiation in those cells.

We first evaluated expression levels of α- and β-syn proteins in the presence of autophagy-lysosomal inhibitors. The results of immunoblot analysis showed that α- and β-syn proteins were up-regulated by macroautophagy inhibitor 3-MA as well as by ammonium chloride, which inhibits lysosomal activity independently of the form of autophagy. By contrast, proteasome inhibitor lactacystin had little effect on the expression of both α- and β-syn proteins (Fig. 8*A*). Thus, these results suggested that α- and β-syn were preferentially degraded by autophagy-lysosomal pathway.

Then, to determine whether down-regulation of autophagy-lysosomal activity affects proteasome function, proteasome activity was evaluated by treatment with autophagy-lysosomal inhibitors. The result showed that treatments with autophagy-lysosomal inhibitors significantly decreased proteasome activities in α-syn-overexpressing cells but not in other cell types (Fig. 8*B*). By contrast, inhibition of proteasome by lactacystin had little effect on cathepsin B activity (data not shown). Similarly, treatment of PMA, which was shown to stimulate proteasome activity (Fig. 6), had little effects on cathepsin B activity (data not shown).

Finally, it was shown that treatment with both 3-MA and ammonium chloride significantly stimulated ALP activity, osteocalcin expression, and matrix mineralization in α-syn-overexpressing cells compared with other cell types (Fig. 8, *C* and *D*, data not shown). Taken together, inhibition of autophagy-lysosomal activity in α-syn-overexpressing cells resulted in down-regulation of proteasome activity, leading to stimulate cellular differentiation. Thus, these results suggest that autophagy-lysosomal pathway may mitigate the down-regulation of proteasome activity by α-syn, therefore leading to abrogate cellular differentiation by α-syn.

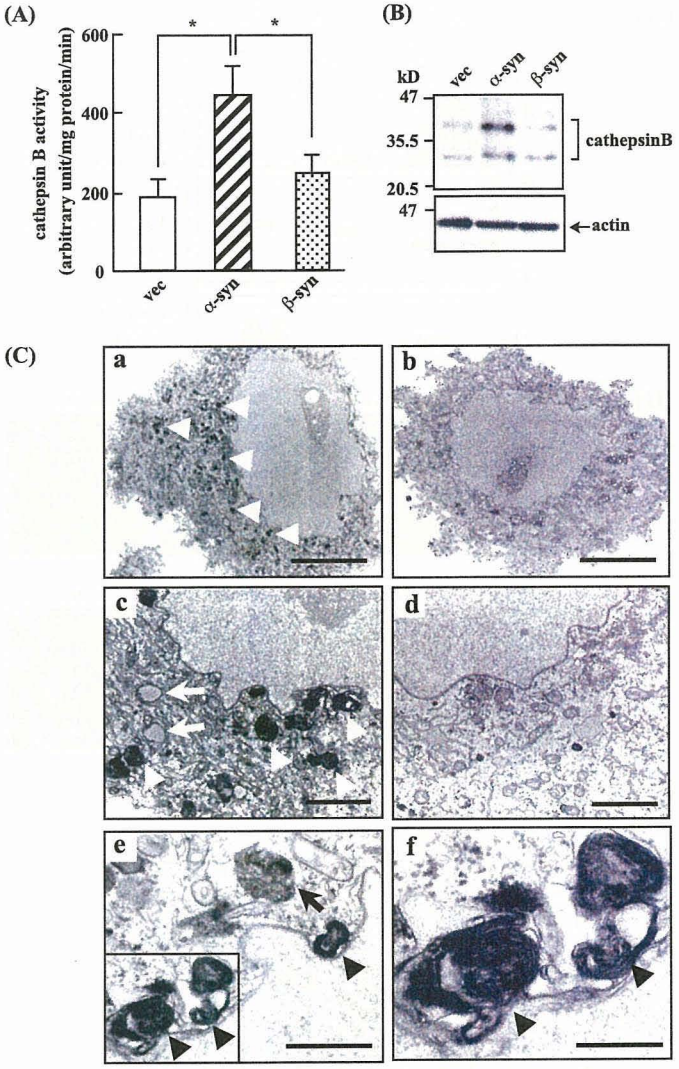

FIGURE 7. **Up-regulation of lysosomal activity in α-syn-overexpressing MG63 cells.** *A*, measurement of cathepsin B activity. Cell extracts (10 μg) were prepared as described under "Experimental Procedures" were analyzed for cathepsin B activity using fluorogenic substrates. Released fluorescence (excitation, 380 nm; emission, 460 nm) was monitored each 5 min up to 60 min. Fluorogenic intensity of each time point was plotted, and slope was calculated. Data shown are the mean ± S.D. ($n = 3$). *, $p < 0.05$; **, $p < 0.01$. *B*, immunoblot analysis of cathepsin B. Cell extracts (v2, α1, and β5) were analyzed by immunoblotting using anti-cathepsin B antibody (*upper panel*) and anti-actin antibody (*lower panel*). *C*, electron microscopic analysis. Typically, α-syn-overexpressing cells (α1: *a*, *c*, *e*, and *f*) exhibited numerous enlarged electron-dense lysosomes (*white arrowheads*), vacuoles that might have already discharged their contents (*white arrows*), autolysosome-like body (*black arrow*), and myelinosome-like structures (*black arrowheads*). The enclosed area in *panel e* is magnified in *panel f*. Fewer lysosomal structures were found in vector-transfected cells (v2, *b*) and β-syn-overexpressing cells (β5, *d*). *Bars* represent 8 μm (*a* and *b*, x1500), 2 μm (*c* and *d*, ×5000), 1 μm (*e*, ×13000), or 0.5 μm (*f*, ×26000).

DISCUSSION

Although α-syn was previously shown to be expressed in the brain tumors that preferentially displayed differentiation rather than proliferation, little has been documented regarding the role of

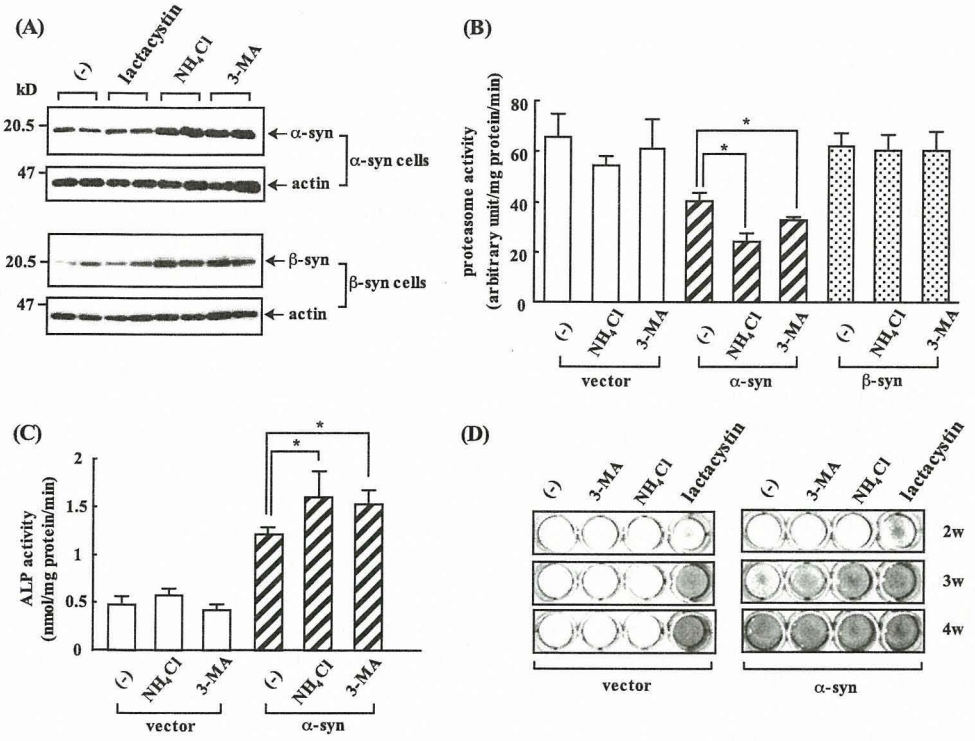

FIGURE 8. **Autophagy-lysosome inhibitor treatment decreases proteasome activity and stimulates cellular differentiation in α-syn-overexpressing MG63 cells.** *A*, immunoblot analysis of syn proteins. Cells (α1, and β5) were incubated under the low serum (0.1%) conditions for 24 h and then treated with 10% serum in the presence of lactacystin (10 μM), ammonium chloride (NH_4Cl) (20 mM), and 3-MA (10 mM) for 24 h. Cell lysates were analyzed by immunoblotting using syn-1 (*upper panel*) and anti-β-syn monoclonal antibody (*low panel*). Blots were reprobed with anti-actin antibody. Similar results were obtained by three independent experiments. *B*, measurement of proteasome activity. Cells (v2, α1, and β5) were prepared as described in *A*. Cell extracts (5 μg) were harvested and incubated with fluorogenic proteasome substrate at 37 °C. Released fluorescence (excitation, 380 nm; emission, 460 nm) was monitored each 5 min up to 60 min. Fluorogenic intensity of each time point was plotted, and slope was calculated. Data shown are the mean ± S.D. ($n = 3$). Please note that proteasome activity was significantly decreased in α-syn-overexpressing cells by ammonium chloride treatment (*, $p < 0.05$). *C*, measurement of ALP activity. Vector-transfected (v2) and α-syn-overexpressing cells (α1) were prepared as described in *A*. Cell extracts at 12 h of treatment were incubated with *p*-nitrophenyl phosphate at 37 °C for 90 min. The amount of released nitrophenol was monitored by the absorbance at 415 nm. Data shown are the mean ± S.D. ($n = 3$). *, $p < 0.05$; **, $p < 0.01$. *D*, *in vitro* mineralization assay. Vector-transfected (v2) and α-syn-overexpressing cells (α1) were treated with ammonium chloride (10 mM), 3-MA, (10 mM), or lactacystin (1 μM) for 2–4 weeks (*2W–4W*). Matrix mineralization was then evaluated by alizarin red staining. Please note that the staining was stimulated by ammonium chloride and to a lesser extent by 3-MA in α-syn-overexpressing cells but not in vector-transfected cells. Similar results were obtained by three independent experiments.

pressing and vector-transfected cells (Fig. 3), it was assumed that down-regulation of proteasome activity by α-syn could be at play for accelerated cellular differentiation in α-syn-overexpressing cells. Supporting this notion, expression levels of p21 were up-regulated due to increased stability at the protein level. Furthermore, high molecular weight proteins with polyubiquitylation were also significantly accumulated (Fig. 3). Thus, it was interpreted that decreased proteasome activity might result in prolonged G_1 phase of cell cycle, which could be prerequisite for proliferating cells to escape from cell cycle and proceed to differentiation. Indeed, it has been well described that proteasome inhibitors stimulated cellular differentiation in a variety of cell types, including osteoblastic cells (45), PC12 cells (46, 47), and oligodendrocytes (48). For example, proteasome inhibitors induced osteoblastic differentiation and bone formation *in vitro* and *in vivo*, which were associated with up-regulation of bone morphogenetic protein-2 (45). It was also shown that proteasome inhibitors stimulated neurite outgrowth in PC12 cells through activation of c-Jun NH_2-terminal kinase signaling pathway (46, 47). We also confirmed that treatment of wild-type MG63 cells with proteasome inhibitors, such as MG132 and lactacystin, resulted in similar differentiation phenotype as characterized by increased expression of p21, up-regulation of ALP and osteocalcin, and enhanced matrix mineralization (Fig. 4).

α-syn for tumor differentiation. The present study showed that α-syn-overexpressing MG63 osteosarcoma cells specifically exhibited phenotype of osteoblastic differentiation. Compared with both β-syn-overexpressing and vector-transfected cells, α-syn-overexpressing cells were characterized by decreased growth rates, associated with increased expression of p21 and reduced phosphorylated Rb (Figs. 1 and 3), indicating that the progression from G_1 to S phase was compromised in these cells. The prolonged G_1 phase would be prerequisite for transition from G_1 to G_0 and subsequent cellular differentiation. Consistent with this view, osteoblastic differentiation markers, including ALP and osteocalcin, were significantly up-regulated in α-syn-overexpressing cells compared with other cell types (Fig. 2). Furthermore, α-syn-overexpressing cells, but not other cell types, were induced to form matrix mineralization during long-term cultures (Fig. 2). Taken together, our results using osteosarcoma cells support the contention that α-syn might stimulate tumor differentiation.

Because proteasome activity was significantly lower in α-syn-overexpressing cells compared with both β-syn-overex-

Then, what is the mechanism through which α-syn suppresses proteasome activity? In this regard several reports have already documented a possibility that α-syn may directly interfere with the proteasome. Based on two-hybrid screening, α-syn was shown to bind to S6′, a component of the 19 S subunit in the 26 S proteasome, in cell cultures (41). Subsequently, it was shown that aggregated α-syn, but not its monomeric form, efficiently inhibited the activity of the 26 S proteasome under the cell-free conditions (42, 43, 49). Using α-syn-overexpressing MG63 cells, we observed that S6a was co-precipitated with α-syn by co-immunoprecipitation experiment, although immunofluorescence/LSCM study revealed that these molecules were partially colocalized in the cytoplasm (Fig. 5). Although we failed to observe any evidence of aggregated α-syn by both immunoblotting and immunofluorescence/LSCM (Fig. 1*B*, *a* and *b*), one possible explanation for supporting the pos-

sibility of the direct suppression of proteasome by α-syn could be that misfolded monomer of α-syn rather than SDS-resistant oligomers/high molecular aggregates might be at play for the suppression of proteasome functions in α-syn-overexpressing MG63 cells. In contrast to α-syn, β-syn, a less aggregate-prone protein that is non-amyloidogenic under the physiological conditions, had little effect on proteasome activity. The result is consistent with the previous report by Snyder *et al.* (49).

An alternative possibility that we favor is that alteration of signal transduction might play an important role for suppression of proteasome activity in α-syn-overexpressing cells. Indeed, it has been shown that various signaling molecules in mitogen-activated protein kinase and phosphatidylinositol 3-kinase pathways were altered by accumulation of α-syn in a variety of cell cultures (35, 50). In the present study the role of the PKC signaling pathway was addressed for the regulation of proteasome activity because it was recently shown that treatment of skeletal muscle with phorbol ester stimulated proteasome activity (39). Consistent with a previous study using neuroblastoma cells and human brains (40), α-syn was shown to bind with PKC, thereby down-regulating the activity of this molecule in α-syn-overexpressing MG63 cells (Fig. 5). Furthermore, treatment of α-syn-overexpressing cells with PMA significantly restored the proteasome activity and abrogated differentiation in these cells (Fig. 6). Thus, proteasome activities were inversely correlated with the extent of differentiation, reinforcing the concept that suppression of proteasome activity by α-syn may accelerate differentiation. Although the precise mechanism by which the proteasome is activated by PKC stimulation requires further investigation, it is possible that phosphorylation might be involved. Supporting this notion, it was recently shown that phosphorylation of α subunits of 20 S proteasome by various stimuli, such as γ-interferon and casein kinase II, was important for the regulation of the stability of 26 S proteasome complexes in mammalian cells (51). Taken together, proteasome activity may be regulated through phosphorylation by signal transduction pathways, including PKC, which may be down-regulated by accumulation of α-syn.

Given the emerging role of autophagy-lysosomal pathway for the degradation of α-syn (52, 53), it is probable that alteration of this pathway may affect α-syn-mediated suppression of proteasome activity. Indeed, the present study showed that the lysosomal activity was significantly up-regulated in α-syn-overexpressing cells compared with other cells (Fig. 7). Furthermore, in α-syn-overexpressing cells, inhibition of the autophagy-lysosomal pathway resulted in down-regulation of proteasome activity associated with up-regulation of α-syn, whereas inhibition of proteasome activity had little effect on autophagy-lysosomal activity with little change of α-syn, suggesting that autophagy-lysosomal pathway is dominant to negatively regulate proteasome activities in these cells (Fig. 8). Together, these results suggest that lysosomal activity was up-regulated due to the compensatory mechanisms against increased level of α-syn. It has been recently shown that the autophagy-lysosomal pathway has pleiotropic roles in the regulation of cancer (54). For example, this pathway may be indispensable to tumors that must frequently survive under the nutrient-poor environments. Conversely, loss of function of this pathway might be beneficial because of accumulation of genotoxic substances in the cytoplasm that could promote mutation and, hence, tumorigenesis. The present study may provide a novel mechanism that the autophagy-lysosomal degradation pathway might negatively modulate the UPS-regulated cellular differentiation in α-syn-overexpressing tumors.

Because the identification of gene mutations of parkin in recessive familial PD and further characterization of this molecule as a ubiquitin E3 ligase, it has been extensively shown that dysfunction of UPS may be one major pathogenic pathway for PD and related neurodegenerative disorders. In this context, much literature has described that overexpression of α-syn was shown to result in decreased proteasome activities in a variety of biological system, including yeast (55) and the inducible expression system in PC12 cells (56), whereas some studies described that suppression of proteasome activity was not observed either in transgenic mice or in some cell cultures, including PC12 and 293 cells (37). Our results are in line with the former reports and further suggest that down-regulation of UPS by α-syn may play an important role for cells to escape from cell cycle and commit to cellular differentiation. Although little has been documented regarding the role of α-syn for cell cycle, Lee *et al.* (57) previously showed that inducible expression of α-syn in PC12 cells resulted in enhanced proliferation rates through stimulation of ERK pathway whereby cells were enriched in the S phase associated with increased accumulation of cyclin B and down-regulation of Rb (57). The reason for the apparent discrepancy between the report by Lee *et al.* (57) and our present study is obscure. However, one possible explanation is that effects of α-syn on growth and differentiation might be cell type-specific. Indeed, it was shown that inducible expression of α-syn in neuro2A cells resulted in inactivation of ERK and other mitogen-activated protein kinase signals (58). Taken together, although our results using MG63 osteosarcoma cells suggest a role of α-syn for tumor differentiation, further investigation is required to confirm our current findings *in vivo*.

In conclusion, our results showed that accumulation of α-syn might result in down-regulation of proteasome activity, leading to accelerate cellular differentiation in osteosarcoma cells. This process is further modulated by various factors, including PKC signaling pathway as well as autophagy-lysosomal activity. Moreover, because a recent study has shown that many of other PD-related molecules are directly or indirectly involved in the regulation of UPS (59), it is possible that the PD-related molecules might converge to regulate the activity of UPS in tumor differentiation. Thus, comprehensive understanding of the common pathway shared by both neurodegenerative disease and cancer have a great potential to provide a novel insight into the mechanism of these distinct categories of diseases.

Acknowledgments—We thank Dr. Koji Okamoto (National Cancer Center Research Institute, Tokyo) for critical reading of the manuscript and Drs. Hidetaka Yakura and Kazuya Mizuno (Tokyo Metropolitan Institute for Neuroscience) for instructions on flow cytometry. We are also indebted to Hideki Itabashi for help in preparing the photographs.

REFERENCES

1. Hashimoto, M., and Masliah, E. (1999) *Brain Pathol.* **9,** 707–720
2. Trojanowski, J., Goedert, M., Iwatsubo, T., and Lee, V. (1998) *Cell Death Differ.* **5,** 832–837
3. Jakes, R., Spillantini, M., and Goedert, M. (1994) *FEBS Lett.* **345,** 27–32
4. Ueda, K., Fukushima, H., Masliah, E., Xia, Y., Iwai, A., Yoshimoto, M., Otero, D. A., Kondo, J., Ihara, Y., and Saitoh, T. (1993) *Proc. Natl. Acad. Sci. U. S. A.* **90,** 11282–11286
5. Lansbury, P. T., Jr. (1999) *Proc. Natl. Acad. Sci. U. S. A.* **96,** 3342–3344
6. Polymeropoulos, M. H., Lavedan, C., Leroy, E., Ide, S. E., Dehejia, A., Dutra, A., Pike, B., Root, H., Rubenstein, J., Boyer, R., Stenroos, E. S., Chandrasekharappa, S., Athanassiadou, A., Papapetropoulos, T., Johnson, W. G., Lazzarini, A. M., Duvoisin, R. C., Di Iorio, G., Golbe, L. I., and Nussbaum, R. L. (1997) *Science* **276,** 2045–2047
7. Kruger, R., Kuhn, W., Muller, T., Woitalla, D., Graeber, M., Kosel, S., Przuntek, H., Epplen, J. T., Schols, L., and Riess, O. (1998) *Nat. Genet.* **18,** 106–108
8. Zarranz, J. J., Alegre, J., Gomez-Esteban, J. C., Lezcano, E., Ros, R., Ampuero, I., Vidal, L., Hoenicka, J., Rodriguez, O., Atares, B., Llorens, V., Gomez Tortosa, E., del Ser, T., Munoz, D. G., and de Yebenes, J. G. (2004) *Ann. Neurol.* **55,** 164–173
9. Hashimoto, M., Rockenstein, E., Mante, M., Mallory, M., and Masliah, E. (2001) *Neuron* **32,** 213–223
10. Park, J. Y., and Lansbury, P. T., Jr. (2003) *Biochemistry* **42,** 3696–3700
11. Ji, H., Liu, Y. E., Jia, T., Wang, M., Liu, J., Xiao, G., Joseph, B. K., Rosen, C., and Shi, Y. E. (1997) *Cancer Res.* **57,** 759–764
12. Lavedan, C., Leroy, E., Dehejia, A., Buchholtz, S., Dutra, A., Nussbaum, R. L., and Polymeropoulos, M. H. (1998) *Hum. Genet.* **103,** 106–112
13. Zhao, W., Liu, H., Liu, W., Wu, Y., Chen, W., Jiang, B., Zhou, Y., Xue, R., Luo, C., Wang, L., Jiang, J. D., and Liu, J. (2006) *Int. J. Oncol.* **28,** 1081–1088
14. Li, Z., Sclabas, G. M., Peng, B., Hess, K. R., Abbruzzese, J. L., Evans, D. B., and Chiao, P. J. (2004) *Cancer* **101,** 58–65
15. Iwaki, H., Kageyama, S., Isono, T., Wakabayashi, Y., Okada, Y., Yoshimura, K., Terai, A., Arai, Y., Iwamura, H., Kawakita, M., and Yoshiki, T. (2004) *Cancer Sci.* **95,** 955–961
16. Jia, T., Liu, Y. E., Liu, J., and Shi, Y. E. (1999) *Cancer Res.* **59,** 742–747
17. Liu, H., Liu, W., Wu, Y., Zhou, Y., Xue, R., Luo, C., Wang, L., Zhao, W., Jiang, J. D., and Liu, J. (2005) *Cancer Res.* **65,** 7635–7643
18. Gupta, A., Inaba, S., Wong, O. K., Fang, G., and Liu, J. (2003) *Oncogene* **22,** 7593–7599
19. Inaba, S., Li, C., Shi, Y. E., Song, D. Q., Jiang, J. D., and Liu, J. (2005) *Breast Cancer Res. Treat.* **94,** 25–35
20. Jiang, Y., Liu, Y. E., Lu, A., Gupta, A., Goldberg, I. D., Liu, J., and Shi, Y. E. (2003) *Cancer Res.* **63,** 3899–3903
21. West, A. B., Dawson, V. L., and Dawson, T. M. (2005) *Trends Neurosci.* **28,** 348–352
22. Wang, F., Denison, S., Lai, J. P., Philips, L. A., Montoya, D., Kock, N., Schule, B., Klein, C., Shridhar, V., Roberts, L. R., and Smith, D. I. (2004) *Genes Chromosomes Cancer* **40,** 85–96
23. Picchio, M. C., Martin, E. S., Cesari, R., Calin, G. A., Yendamuri, S., Kuroki, T., Pentimalli, F., Sarti, M., Yoder, K., Kaiser, L. R., Fishel, R., and Croce, C. M. (2004) *Clin. Cancer Res.* **10,** 2720–2724
24. Liu, Y., Lashuel, H. A., Choi, S., Xing, X., Case, A., Ni, J., Yeh, L. A., Cuny, G. D., Stein, R. L., and Lansbury, P. T., Jr. (2003) *Chem. Biol.* **10,** 837–846
25. Caballero, O. L., Resto, V., Patturajan, M., Meerzaman, D., Guo, M. Z., Engles, J., Yochem, R., Ratovitski, E., Sidransky, D., and Jen, J. (2002) *Oncogene* **21,** 3003–3010
26. Nagakubo, D., Taira, T., Kitaura, H., Ikeda, M., Tamai, K., Iguchi-Ariga, S. M., and Ariga, H. (1997) *Biochem. Biophys. Res. Commun.* **231,** 509–513
27. Kim, R. H., Peters, M., Jang, Y., Shi, W., Pintilie, M., Fletcher, G. C., DeLuca, C., Liepa, J., Zhou, L., Snow, B., Binari, R. C., Manoukian, A. S., Bray, M. R., Liu, F. F., Tsao, M. S., and Mak, T. W. (2005) *Cancer Cell* **7,** 263–273
28. Kawashima, M., Suzuki, S. O., Doh-ura, K., and Iwaki, T. (2000) *Acta Neuropathol. (Berl.)* **99,** 154–160
29. Fung, K. M., Rorke, L. B., Giasson, B., Lee, V. M., and Trojanowski, J. Q. (2003) *Acta Neuropathol. (Berl.)* **106,** 167–175
30. Bruening, W., Giasson, B. I., Klein-Szanto, A. J., Lee, V. M., Trojanowski, J. Q., and Godwin, A. K. (2000) *Cancer* **88,** 2154–2163
31. Hashimoto, M., Yoshimoto, M., Sisk, A., Hsu, L. J., Sundsmo, M., Kittel, A., Saitoh, T., Miller, A., and Masliah, E. (1997) *Biochem. Biophys. Res. Commun.* **237,** 611–616
32. Stefanis, L., Kholodilov, N., Rideout, H. J., Burke, R. E., and Greene, L. A. (2001) *J. Neurochem.* **76,** 1165–1176
33. Takeda, A., Hashimoto, M., Mallory, M., Sundsumo, M., Hansen, L., and Masliah, E. (2000) *Acta Neuropathol. (Berl)* **99,** 296–304
34. Takenouchi, T., Hashimoto, M., Hsu, L. J., Mackowski, B., Rockenstein, E., Mallory, M., and Masliah, E. (2001) *Mol. Cell. Neurosci.* **17,** 141–150
35. Hashimoto, M., Takenouchi, T., Rockenstein, E., and Masliah, E. (2003) *J. Neurochem.* **85,** 1468–1479
36. Tanimoto, Y., Yokozeki, M., Hiura, K., Matsumoto, K., Nakanishi, H., Matsumoto, T., Marie, P. J., and Moriyama, K. (2004) *J. Biol. Chem.* **279,** 45926–45934
37. Martin-Clemente, B., Alvarez-Castelao, B., Mayo, I., Sierra, A. B., Diaz, V., Milan, M., Farinas, I., Gomez-Isla, T., Ferrer, I., and Castano, J. G. (2004) *J. Biol. Chem.* **279,** 52984–52990
38. Nakai, M., Toshimori, K., Yoshinaga, K., Nasu, T., and Hess, R. A. (1998) *Cell Tissue Res.* **294,** 145–152
39. Wyke, S. M., and Tisdale, M. J. (2006) *Life Sci.* **78,** 2898–2910
40. Ostrerova, N., Petrucelli, L., Farrer, M., Mehta, M., Choi, P., Hardy, J., and Wolozin, B. (1999) *J. Neurosci.* **19,** 5782–5791
41. Ghee, M., Fournier, A., and Mallet, J. (2000) *J. Neurochem.* **75,** 2221–2224
42. Snyder, H., Mensah, K., Theisler, C., Lee, J., Matouschek, A., and Wolozin, B. (2003) *J. Biol. Chem.* **278,** 11753–11759
43. Lindersson, E., Beedholm, R., Hojrup, P., Moos, T., Gai, W., Hendil, K. B., and Jensen, P. H. (2004) *J. Biol. Chem.* **279,** 12924–12934
44. Rubinsztein, D. C. (2006) *Nature* **443,** 780–786
45. Garrett, I. R., Chen, D., Gutierrez, G., Zhao, M., Escobedo, A., Rossini, G., Harris, S. E., Gallwitz, W., Kim, K. B., Hu, S., Crews, C. M., and Mundy, G. R. (2003) *J. Clin. Investig.* **111,** 1771–1782
46. Obin, M., Mesco, E., Gong, X., Haas, A. L., Joseph, J., and Taylor, A. (1999) *J. Biol. Chem.* **274,** 11789–11795
47. Giasson, B. I., Bruening, W., Durham, H. D., and Mushynski, W. E. (1999) *J. Neurochem.* **72,** 1081–1087
48. Pasquini, L. A., Paez, P. M., Moreno, M. A., Pasquini, J. M., and Soto, E. F. (2003) *J. Neurosci.* **23,** 4635–4644
49. Snyder, H., Mensah, K., Hsu, C., Hashimoto, M., Surgucheva, I. G., Festoff, B., Surguchov, A., Masliah, E., Matouschek, A., and Wolozin, B. (2005) *J. Biol. Chem.* **280,** 7562–7569
50. Seo, J. H., Rah, J. C., Choi, S. H., Shin, J. K., Min, K., Kim, H. S., Park, C. H., Kim, S., Kim, E. M., Lee, S. H., Lee, S., Suh, S. W., and Suh, Y. H. (2002) *FASEB J.* **16,** 1826–1828
51. Bose, S., Stratford, F. L., Broadfoot, K. I., Mason, G. G., and Rivett, A. J. (2004) *Biochem. J.* **378,** 177–184
52. Webb, J. L., Ravikumar, B., Atkins, J., Skepper, J. N., and Rubinsztein, D. C. (2003) *J. Biol. Chem.* **278,** 25009–25013
53. Cuervo, A. M., Stefanis, L., Fredenburg, R., Lansbury, P. T., and Sulzer, D. (2004) *Science* **305,** 1292–1295
54. Mizushima, N. (2005) *Cell Death Differ.* **12,** Suppl. 2, 1535–1541
55. Chen, Q., Thorpe, J., and Keller, J. N. (2005) *J. Biol. Chem.* **280,** 30009–30017
56. Tanaka, Y., Engelender, S., Igarashi, S., Rao, R. K., Wanner, T., Tanzi, R. E., Sawa, A., V. L. D., Dawson, T. M., and Ross, C. A. (2001) *Hum. Mol. Genet.* **10,** 919–926
57. Lee, S. S., Kim, Y. M., Junn, E., Lee, G., Park, K. H., Tanaka, M., Ronchetti, R. D., Quezado, M. M., and Mouradian, M. M. (2003) *Neurobiol. Aging* **24,** 687–696
58. Iwata, A., Maruyama, M., Kanazawa, I., and Nukina, N. (2001) *J. Biol. Chem.* **276,** 45320–45329
59. Abou-Sleiman, P. M., Muqit, M. M., and Wood, N. W. (2006) *Nat. Rev. Neurosci.* **7,** 207–219

ELSEVIER

Bone 40 (2007) 997–1005

BONE

www.elsevier.com/locate/bone

Association of a single-nucleotide variation (A1330V) in the low-density lipoprotein receptor-related protein 5 gene (*LRP5*) with bone mineral density in adult Japanese women

Yoichi Ezura [a,*], Toshiaki Nakajima [a], Tomohiko Urano [b], Yoshihiro Sudo [a], Mitsuko Kajita [a], Hideyo Yoshida [c], Takao Suzuki [c], Takayuki Hosoi [d], Satoshi Inoue [b], Masataka Shiraki [e], Mitsuru Emi [a]

[a] *Department of Molecular Biology, Institute of Gerontology, Nippon Medical School, 1-396, Kosugi-cho, Nakahara-ku, Kawasaki 211-8533, Japan*
[b] *Department Geriatric Medicine, Faculty of Medicine, University of Tokyo, Tokyo, Japan*
[c] *Department Epidemiology, Tokyo Metropolitan Institute of Gerontology, Tokyo, Japan*
[d] *Department Internal Medicine, Tokyo Metropolitan Geriatric Hospital, Tokyo, Japan*
[e] *Research Institute and Practice for Involutional Diseases, Nagano, Japan*

Received 20 October 2004; revised 29 May 2005; accepted 13 June 2005
Available online 15 February 2007

Abstract

Low-density lipoprotein receptor-related protein 5 (LRP5), a co-receptor of Wnt signaling, is an important regulator of bone development and maintenance. Recently we identified correlation between an intronic single-nucleotide polymorphism (SNP) in the *LRP5* gene and vertebral bone mineral density (BMD), indicating that a genetic ground exists at this locus for determination of BMD. In the study reported here, we searched for nucleotide variation(s) that might confer susceptibility to osteoporosis among an extended panel of 387 healthy subjects recruited from the same hospital (Group-A), as well as among 384 subjects from the general population in eastern Japan (Group-B). We basically focused on two potentially functional variations, Q89R (c.266A > G) and A1330V (c.3989C > T), whose functional effects by the amino-acid changes were estimated by the SIFT software program; it predicted the 1330 V allele as deleterious ("intolerant") although the minor allele of Q89R was questionable. By analyzing associations between the variant alleles and the BMD, reproducible association of the minor variant of A1330V to lower adjusted BMD levels was detected; i.e., In Group-A subjects 1330-V significantly associated with the spinal BMD *Z*-score ($P = 0.034$), and in Group-B it associated with low radial BMD ($P = 0.019$). From haplotype and linkage disequilibrium (LD) analysis for 29 SNPs, we detected two separate LD blocks within the entire 137-kb *LRP5* locus, basically consistent with a previous report on Caucasians. One of the second block haplotype significantly associated with adjusted BMD ($r = 0.15$, $P = 0.004$). Possible combined effect of Q89R and A1330V belonging to different LD blocks was denied by multiple regression analyses. Our results indicate that genetic variations in *LRP5* are important factors affecting BMD in adult women and that 1330 V may contribute to osteoporosis susceptibility, at least in Japanese.

Keywords: Single-nucleotide polymorphism; LRP5; Low-density lipoprotein receptor-related protein; Bone mineral density; Association study; Quantitative trait

Introduction

Osteoporosis is a common, multi-factorial disease characterized by reduced bone mass, microarchitectual deterioration of bone tissue, and increased risk of fragility fractures. Achievement of high peak bone mass before maturation, as well as avoidance of postmenopausal bone loss, is important for prevention of osteoporosis [1]. Since complicated processes during periods of development, maturation, and aging are regulated through multiple endocrine and local systems, many aspects of the mechanisms affecting control of bone mass remain to be clarified.

Wnt signaling is likely to be one of the most important systems involved in regulating developmental and homeostatic control of the skeletal system [2–4]. Low-density lipoprotein receptor-related protein 5 (LRP5) is a co-receptor for Wnt [5,6],

* Corresponding author. Present address: 2-3-10 Kanda-Surugadai, Chiyoda-ku, Tokyo, Tokyo Medical and Dental University, Medical Research Institute, Department of Molecular Pharmacology. Fax: +81 3 5280 8067.
E-mail address: ezura.mph@mri.tmd.ac.jp (Y. Ezura).

8756-3282/$ - see front matter © 2007 Published by Elsevier Inc.
doi:10.1016/j.bone.2005.06.025

and by studies on osteoporosis pseudoglioma syndrome (OPPG) family, causative mutations were identified in the *LRP5* gene [7,8]. On the other hand, certain mutations in *LRP5* cause an inherited trait of high bone mass in some families [9,10], and autosomal-dominant osteopetrosis in others [11]. These observations strongly suggest an important general role of LRP5 in acquisition and/or maintenance bone mass.

Genes responsible for monogenic inherited diseases sometimes also play roles in the phenotypic manifestations of common diseases [12–14], and thus are first-choice candidates for testing associations. Previously we suggested a possible contribution of LRP5 in determination of BMD, after detecting an intronic nucleotide variation of the *LRP5* gene (IVS17-1677C > A) associated with age-adjusted values of spinal BMD (*Z*-score) in a set of adult Japanese women. Although no definitive responsible variation(s) were established at that time [15], three other groups subsequently reported association of different missense nucleotide variations in *LRP5* with bone mineral density among Asian populations (Korean and Japanese; Q89R and A1330V [16,17]) and in Caucasians (V667M [18]). Although the significance levels and the suggested responsible variations were different, the reports were consistent in implicating the *LRP5* locus.

To examine in more detail the possibly responsible variation(s) of that gene in terms of BMD, we investigated multiple genetic variations within the *LRP5* locus in two independently recruited subject groups, comprising a total of 771 adult women in Japan. We constructed haplotypes, analyzed linkage disequilibrium (LD), and searched for mutations in these subjects.

Materials and methods

Subjects

The 308 subjects recruited for the previous report [15] were from an outpatient clinic in Nagano prefecture (Research Institute and Practice for Involutional Diseases). Although BMD levels distributed in a wide range without skewness, these subjects were not from a population-based panel, and thus adjustment by multiple regression was not applicable. However instead, quantitative association analysis was possible using spinal BMD *Z*-scores, and we detected significant association with an intronic variant of *LRP5*. To verify that association, extended panel of 387 adult female was recruited from the same clinic (Group-A); these are basically healthy individuals who visited the same clinic up to December 2003. Mean ages and body mass indices (BMI) with standard deviations (SD) were 64.6 ± 10.8 (range 25–89) years and 22.2 ± 2.9 (range 14.3–32.9) kg/m^2, respectively. The BMD of lumbar vertebral bodies (from L2 to L4; expressed in g/cm^2) was measured in each participant by DXA using DPX-L (GE Medical Systems Lunar Corporation, Madison WI). Coefficients of variation (CV) for the anteroposterior view of the lumbar BMD was 0.5 ± 0.5% (CV ± SD) as described [40]. *Z*-scores were calculated using installed software (Lunar DPX-L) on the basis of data from 20,000 Japanese women [19]. Eight of the subjects had remarkably high BMD (*Z*-scores > 3.0),

Table 1
Summary of LRP5 polymorphisms analyzed among 384 adult women in the general Japanese population

No.	SNP name	nt.	cSNP characteristics †	dbSNP-ID ‡	Allele frequency (%-Heterozygosity)	*n* §	Distance (bp) *	Genotyping method
1	IVS1 + 4689C > G	G/C		rs312014	0.53:0.47 (45)	378	9469	TaqMan
2	IVS1 + 14158G > A	G/A		rs312024	0.44:0.56 (46)	383	310	Invader
3	IVS1 + 14468T > C	T/C		rs634008	0.26:0.74 (41)	367	7259	Sd-PCR
4	IVS1-13315A > G	G/A		rs606989	0.91:0.09 (16)	378	9089	TaqMan
5	IVS1-4226T/C	T/C		rs74744	0.09:0.91 (18)	384	3832	Invader
6	IVS1-394A/G	A/G		rs312782	0.09:0.91 (17)	369	567	Sd-PCR
7	Q89R	A/G	(c.266A > G)	–	0.93:0.07 (13)	383	3075	Invader
8	IVS2 + 2852T > C	T/C		rs312783	0.09:0.91 (18)	381	197	Sd-PCR
9	IVS2 + 3049T > C	T/C		rs312784	0.11:0.89 (21)	375	3535	Sd-PCR
10	IVS2 + 2823T > G	T/G		rs312788	0.09:0.91 (18)	384	9317	Invader
11	IVS4 + 201G > A	A/G		rs178352	0.91:0.09 (18)	377	21,779	TaqMan
12	IVS5-393C > T	C/T		rs3781592	0.06:0.94 (11)	381	5761	Sd-PCR
13	IVS7 + 1632G > A	G/A		rs3781590	0.09:0.91 (16)	374	11,224	Invader
14	IVS7-575T > C	T/C		rs685095	0.30:0.70 (40)	382	7134	Sd-PCR
15	c.2220C > T	C/T	Silent	rs2306862	0.26:0.74 (36)	372	218	Sd-PCR
16	IVS10 + 120T > C			rs667126	0.30:0.70 (40)	384	907	Invader
17	IVS10-269C > T	C/T		rs583545	0.33:0.67 (45)	370	33	Sd-PCR
18	IVS10-236A > G	A/G		rs23691	0.34:0.66 (42)	381	498	Invader
19	IVS11 + 78G > A	G/A		rs689179	0.30:0.70 (41)	378	13,524	Sd-PCR
20	c.3357A > G	A/G	Silent	rs556442	0.42:0.58 (51)	373	6662	Sd-PCR
21	IVS17-1718G/del	G/del		rs3837372	0.39:0.61 (46)	383	41	Invader
22	IVS17-1677C > A	C/A		rs3781586	0.28:0.72 (41)	375	941	Sd-PCR
23	IVS17-376G > A	G/A		rs3781585	0.05:0.95 (10)	379	110	Sd-PCR
24	IVS17-626G > A	G/A		rs3781584	0.05:0.95 (10)	383	101	Invader
25	IVS17-525C > T	C/T		rs3781583	0.05:0.95 (10)	384	750	Invader
26	A1330V	C/T	(c.3989C > T)	rs3736228	0.26:0.71 (40)	384	1285	Invader
27	IVS18 + 1274A > G	A/G		rs638076	0.39:0.61 (44)	377	2998	Sd-PCR
28	IVS19-336T > C	T/C		rs901823	0.36:0.64 (44)	370	4140	Sd-PCR
29	IVS21 + 2334T > C	T/C		rs3781579	0.19:0.83 (28)	375	–	Sd-PCR

* Number of nucleotides to the next SNP (bp).
† Nucleotide positions in the coding sequence are indicated for missense cSNPs.
‡ IDs are from dbSNP of NCBI (http://www.ncbi.nlm.nih.gov/SNP/).
§ Number of genotyped subjects.